

1 **Increasing concentrations of dichloromethane, CH₂Cl₂, inferred from CARIBIC air samples**
2 **collected 1998-2012**

3
4 E. C. Leedham Elvidge¹, D. E. Oram^{2,3}, J. C. Laube², A. K. Baker¹, S. A. Montzka⁴, S. Humphrey²,
5 D. A. O'Sullivan^{2,5} and C. A. M. Brenninkmeijer¹

6
7 ¹ CARIBIC, Max Plank Institute for Chemistry, Hahn-Meitner Weg 1, 55128 Mainz, Germany

8 ² Centre for Ocean and Atmospheric Sciences, School of Environmental Sciences, University of
9 East Anglia, Norwich Research Park, Norwich, NR4 7TJ, UK

10 ³ National Centre for Atmospheric Science, University of East Anglia, Norwich, NR4 7TJ, UK

11 ⁴ National Oceanic and Atmospheric Administration, Boulder, CO, 80304, USA

12 ⁵ now at Met Office, FitzRoy road, Exeter, EX1 3PB

13 Correspondence to E. Leedham (emma.leedham@mpic.de)

14
15 **Abstract**

16 Atmospheric concentrations of dichloromethane, CH₂Cl₂, a regulated toxic air pollutant and minor
17 contributor to stratospheric ozone depletion, were reported to have peaked around 1990 and to be
18 declining in the early part of the 21st century. Recent observations suggest this trend has reversed
19 and CH₂Cl₂ is once again increasing in the atmosphere. Despite the importance of ongoing
20 monitoring and reporting of atmospheric CH₂Cl₂, no time series has been discussed in detail since
21 2006. The CARIBIC project (Civil Aircraft for the Regular Investigation of the atmosphere Based
22 on an Instrument Container) has analysed the halocarbon content of whole air samples collected at
23 altitudes of between ~10-12 km via a custom-built container installed on commercial passenger
24 aircraft since 1998, providing a long-term record of CH₂Cl₂ observations. In this paper we present
25 this unique CH₂Cl₂ time series, discussing key flight routes which have been used at various times
26 over the past 15 years. Between 1998 and 2012 increases were seen in all northern hemispheric
27 regions and at different altitudes, ranging from ~7-10 ppt in background air to ~13-15 ppt in regions
28 with stronger emissions (equating to a 38-69% increase). Of particular interest is the rising
29 importance of India as a source of atmospheric CH₂Cl₂: based on CARIBIC data we provide
30 regional emission estimates for the Indian subcontinent and show that regional emissions have
31 increased from 3-14 Gg yr⁻¹ (1998-2000) to 16-25 Gg yr⁻¹ (2008). Potential causes of the increasing
32 atmospheric burden of CH₂Cl₂ are discussed. One possible source is the increased use of CH₂Cl₂ as
33 a feedstock for the production of HFC-32, a chemical used predominantly as a replacement for
34 ozone-depleting substances in a variety of applications including air conditioners and refrigeration.

36

37 **1. Introduction**

38

39 Dichloromethane, CH_2Cl_2 , is a short-lived chlorocarbon of mainly (up to 90% (Montzka et al.,
40 2011b)) anthropogenic origin. Its main applications include use in paint strippers, degreasers and
41 solvents; in foam production and blowing applications; as a chemical feedstock; and as an
42 agricultural fumigant (Montzka et al., 2011b). The contribution from natural sources (mainly
43 biomass burning and an oceanic source) is uncertain. Simmonds et al. (2006) obtained a good
44 model fit to their observations using a 10% combined oceanic and biomass burning source,
45 although they showed that a stronger terrestrial source could support natural emissions of up to
46 30%. However, recent field measurements of biomass burning plumes have indicated that this
47 source is likely to be smaller than previously estimated (Simpson et al., 2011). With an atmospheric
48 lifetime of around 5 months (Montzka et al., 2011b), CH_2Cl_2 displays significant atmospheric
49 spatial variations and temporal trends. Its seasonal cycle is mainly due to reaction with the OH
50 radical, with maxima in late winter/early spring and corresponding minima in late summer or early
51 autumn (Cox et al., 2003). There are no discernible seasonal variations in emissions or end uses
52 (Gentner et al., 2010; McCulloch and Midgley, 1996). Significantly higher concentrations are
53 observed in the northern hemisphere (NH, southern hemisphere = SH) due to the predominant
54 industrial source. A NH:SH mole fraction ratio of 2.7 has been reported for the lower troposphere
55 (Simmonds et al., 2006).

56

57 Short-lived chlorocarbons, including CH_2Cl_2 , contribute to stratospheric chlorine and its cycling
58 with stratospheric ozone. Their current contribution is minor, Laube et al. (2008) found that at 15.2
59 km (the level of zero radiative heating) 1.4% of chlorine from organic compounds was from short-
60 lived chlorocarbons, of which half was from CH_2Cl_2 . This level is important because air parcels at
61 or above this level point are likely to be transported to the stratosphere. However, current and
62 projected decreases of longer-lived anthropogenic chlorocarbons (such as CH_3CCl_3 , CCl_4 , halons
63 and CFCs) could mean a greater relative importance of shorter-lived chlorocarbons with respect to
64 stratospheric chlorine, especially if their atmospheric abundances were to increase. Due to its
65 predominantly anthropogenic source CH_2Cl_2 is susceptible to changes in industrial emissions.
66 CH_2Cl_2 is also of concern as it is also a toxic air pollutant and possible carcinogen and, as such, is
67 regulated by national and European Union Law, for example the Solvent Emissions Directive,
68 1999/13/EC (E.C.S.A., 2007).

69

70

71 The earliest reported NH atmospheric measurements of CH₂Cl₂ were made in the mid-1970s and
72 observed concentrations of 35 ±19 ppt (Cox et al., 1976). A range of global measurements in the
73 1980s and 1990s (many of which will be discussed further throughout this manuscript and are
74 included in Table 2, see also Simmonds et al., (2006) for an in-depth discussion of many of the
75 observations during this period) showed a consistent picture of peaking concentrations, with an
76 average of ~30-40 ppt around 1990, followed by a decline linked to decreasing industrial use of
77 CH₂Cl₂ (McCulloch et al., 1999). Measurements made between 1989 and 1996 at Alert, Canadian
78 Arctic, observed a decline of around -4% (-1.8 ppt) per year (Gautrois et al., 2003). Long-term
79 measurements (1995-2004) at Mace Head, Ireland demonstrated a decline in CH₂Cl₂ pollution
80 events since measurements began in 1995, although this decline had stabilised in the later years of
81 the dataset (Simmonds et al., 2006). In the SH, Advanced Global Atmospheric Gases Experiment
82 (AGAGE) atmospheric measurements began at Cape Grim in 1998 and reported mean CH₂Cl₂
83 concentrations for 1998-2000 of 8.9 (±0.2) ppt (Cox et al., 2003). These early measurements were
84 supported by firm records which indicated that SH CH₂Cl₂ concentrations increased from 1-2 ppt at
85 the beginning of the record (pre-1940) to 9 ppt around 1990 (Trudinger et al., 2004). Due to the lack
86 of industrial emissions in the SH the rapid decline in atmospheric concentrations seen in the NH
87 was not observed in the AGAGE Cape Grim time series (Simmonds et al., 2006).

88

89 In recent years increasing CH₂Cl₂ concentrations have been observed in both the NH and SH.
90 Montzka et al. (2011b) reported an increase of around 8% between 2007 and 2008, based on
91 updated AGAGE data from Simmonds et al. (2006). There was no corresponding increase in
92 CHCl₃, 70% of which is believed to be of natural origin (Worton et al., 2006). The increase was
93 also noted in Montzka et al. (2011a, see their Supplementary Information) whose time series of
94 CH₂Cl₂ between 1995 to 2009 shows increasing atmospheric concentrations in recent years.
95 CARIBIC (Civil Aircraft for the Regular Investigation of the atmosphere Based on an Instrument
96 Container) CH₂Cl₂ measurements up to the end of 2012 provide the opportunity to investigate this
97 increase from a global time series perspective and may help improve our understanding of the
98 recent changes in atmospheric CH₂Cl₂.

99

100

101

102

103

104

105

106 **2. Methods**

107

108 **2.1 The CARIBIC platform and whole air samples**

109

110 CARIBIC centres on a large air-freight container accommodating a range of scientific equipment
111 which is deployed monthly aboard a commercial passenger aircraft departing from Germany for up
112 to four consecutive long-haul flights. Details of both CARIBIC phases can be found on our website,
113 caribic-atmospheric.com. CARIBIC phase 1 (CARIBIC1) operated between 1997 and 2002 aboard
114 a Boeing 767 departing for several global destinations from either Düsseldorf or Munich airport.

115 Whole air samples were collected using 12 21 l stainless steel tanks pressurised to 17 bar. Details of
116 CARIBIC1, including the range of other measurements made, can be found in Brenninkmeijer et al.
117 (1999). Halocarbon data are available for 1998-2002.

118

119 Between 2003 and 2005 a new container was developed and this system was deployed aboard a
120 Lufthansa Airbus 340-600 departing from Frankfurt Airport. CARIBIC phase 2 (CARIBIC2) began
121 in 2005 and, at the time of writing, is still in operation. Samples are taken en route to destinations
122 across the globe with flights occurring approximately monthly. Two whole air samplers consisting
123 of 14 2.7 l glass flasks collect 28 air samples for halocarbon, non-methane hydrocarbon (NMHCs)
124 and greenhouse gas measurements at pre-determined intervals during the flight, mainly within
125 cruising altitudes of around 10-12 km. Filling times are between 30-90 s, averaging 45 s or 10 km
126 of the flight path. Further air sampler information can be found in Baker et al. (2010) and Schuck et
127 al. (2009). The fully-automated CARIBIC2 system contains a range of other sampling equipment,
128 including, but not limited to, equipment for the in-situ or post-flight analysis of ozone (O₃), carbon
129 monoxide (CO), aerosols and water vapour. Further information can be found in Brenninkmeijer et
130 al. (2007).

131

132

133

134

135

136

137

138

139

140

141 2.2 Halocarbon analysis

142

143 During both CARIBIC1 and CARIBIC2 air samples were sent to the University of East Anglia
144 (UEA, UK) for halocarbon analysis via gas chromatography mass spectrometry (GCMS). During
145 CARIBIC1 subsamples were removed from the main canisters into electropolished stainless steel
146 cans and sent to UEA. For CARIBIC2 the whole air sampling units were sent directly to UEA for
147 analysis. During CARIBIC1 two separate GCMS systems were used. The first was an Agilent/HP
148 5890A GC coupled to a double-focusing, tri-sector mass spectrometer (V.G./Micromass Autospec).
149 Each 200 ml air sample was dried by passing through magnesium perchlorate (MPC) before being
150 trapped in a previously evacuated stainless steel loop filled with 100 μm glass beads and immersed
151 in liquid argon ($-186\text{ }^{\circ}\text{C}$). The bulk of the air passed into an evacuated stainless steel flask where the
152 pressure change, and hence sample volume, was measured with a capacitance manometer (Edwards
153 Barocel). The MPC trap was shown to have no effect on the measured CH_2Cl_2 concentration.

154 Halocarbons were separated on a 60 m x 0.53 mm (1.5 μm film thickness) DB5 capillary column
155 (J&W), with helium carrier gas (2 ml min^{-1}) and a temperature program of $-20\text{ }^{\circ}\text{C}$ (2 min) rising to
156 $220\text{ }^{\circ}\text{C}$, at a rate of $15\text{ }^{\circ}\text{C min}^{-1}$. The mass spectrometer was operated in selected ion mode (voltage
157 switching) using electron ionisation (EI). Each air sample was analysed at least twice, with a
158 working standard analysed before and after each sample pair to allow correction for small changes
159 in instrument response.

160

161

162

163

164

165

166

167

168

169

170

171

172

173

174

175

176 The V.G. Autospec system was used from the start of analysis at UEA in June 1998 until December
177 1999. In 1999 a new instrument ('Entech') was purchased by UEA and became the main instrument
178 for CARIBIC sample analysis. This system consisted of an Agilent 6890 GC and 5973 quadrupole
179 MS. With this system pre-concentration was achieved using a commercial, fully automated, 3-stage
180 pre-concentrator (Entech Instruments, model 7100). This system was used throughout the rest of
181 CARIBIC1 and CARIBIC2. The Entech pre-concentrator employs multiple traps to remove water
182 (Trap 1), CO₂ (Trap 2) and to cryo-focus the sample prior to injection into the GC (Trap 3).
183 Typically, between 800-1000 ml of air are trapped at 100 ml min⁻¹ onto a 1/8" (external diameter,
184 OD) stainless steel trap (Trap 1) packed with glass beads and held at -150 °C. The contents of Trap
185 1 are then swept onto Trap 2, consisting of 1/8" OD stainless steel packed with Tenax adsorbent and
186 held at -40 °C. Trap 3 cryo-focuses the sample on a fused silica lined stainless steel tube (1/32"
187 OD). Until 2010 a DB-5 capillary column (J&W Scientific, 105 m x 0.32 mm ID, 1.5 µm film
188 thickness) was used for separation. In 2010 the column was changed to an Agilent GC-GasPro
189 column (30 m x 0.32 mm). The temperature program used with the DB-5 column was 30 °C for 8
190 min rising to 220 °C at a rate of 10 °C min⁻¹. The temperature program used with the GasPro
191 column is -10 °C for 2 min rising to 200 °C at a rate of 10 °C min⁻¹. The MS is operated in selected
192 ion mode using EI at 70 eV. The system allows for the unattended analysis of up to 16 samples,
193 interspersed with equal volume aliquots of a working standard analysed at regular intervals. Each
194 sample is normally analysed only once and, as the response of the quadrupole analyser is more
195 stable than the Autospec, the working standard is analysed less frequently.

196

197 To assist with the transition between the V. G. Autospec and the Entech system parallel analysis
198 was conducted for two flights in July 2000. Agreement between the two systems was excellent. Of
199 the 24 samples analysed on both systems all but 5 had a difference of less than ±1 ppt
200 (corresponding to a difference of <3% standard deviation, σ , or less than the precision of these
201 instruments). For the 5 remaining samples the difference was less than ±2 ppt. The CH₂Cl₂ samples
202 that were analysed on both systems were treated in the following manner. If the difference was less
203 than ±1 ppt (3% σ) the values were averaged and the variation between the two measurements
204 incorporated into error bars plotted with these values. Where the difference was greater than ±1 ppt
205 the V.G. Autospec value was selected based on the better precision of this instrument with respect
206 to CH₂Cl₂.

207

208

209

210

211 To provide additional support to the CARIBIC2 dataset, three flights, one per year between 2009-
212 2011, were also analysed on a highly sensitive Waters Autospec magnetic sector GCMS. This
213 system is the direct replacement of the V.G. Autospec described above and, whilst a number of
214 minor modifications have been made to the analytical procedure (see Laube et al., 2010), the system
215 is essentially the same. Where the Entech and Autospec values agreed within $\pm 1\sigma$ (based on
216 replicate Autospec measurements) the values were combined. As with CARIBIC1, these values all
217 agreed within ± 1 ppt. For the remaining samples the values from the higher precision Autospec
218 system have been used. The limit of detection for all 3 analytical systems was 0.1 ppt or better.

219
220 For CH_2Cl_2 the UEA calibration is tied to the 2003 GCMS gravimetric scale of the Global
221 Monitoring Division of the Earth System Research Laboratory of the National Oceanic and
222 Atmospheric Administration (NOAA-ESRL-GMD) in Boulder, CO, USA. A number of calibrated,
223 high pressure whole-air samples collected at Niwot Ridge (a remote site near Boulder) were
224 acquired between 1994 and 2009. These were used for the propagation of mixing ratios to all
225 CARIBIC measurements. Further details on this procedure can be found in the Supplementary
226 Material. The CH_2Cl_2 data are reported on the latest (2003) NOAA-ESRL calibration scale. NOAA
227 do not provide an absolute accuracy on their calibrated gas standards but, in a recent international
228 comparison exercise (IHALACE), the mean of the CH_2Cl_2 calibration scales from the three
229 independent calibration laboratories was found to have a standard deviation of $\pm 9\%$ (Hall et al.
230 2014). In Section 3.1, CARIBIC data are compared to the long term CH_2Cl_2 record from Mace
231 Head (53.3°N , 9.9°W , 42 m above sea level) measured by NOAA-ESRL-GMD. These data are
232 obtained from regularly collected flask samples analysed by GCMS. Sampling at Mace Head is
233 done in a manner to characterise only air that is arriving from the clean air sector, specifically when
234 wind direction is between 180° to 320° and the wind speed is greater than 4m s^{-1} . For further
235 information see Montzka et al. (2011a) and <http://www.esrl.noaa.gov/gmd/hats/gases/CH2Cl2.html>.
236 A comparison between NOAA and UEA calibration scales is discussed in the Supplementary
237 Information which provides a comparison of data from Cape Grim, a ground-based site sampled by
238 both groups. Cape Grim samples analysed by both groups compare well (65% agree within the
239 respective 1 sigma standard deviations), with no apparent offset or change in the relationship
240 between both groups' results over time (NOAA/UEA ratio of 1.02 ± 0.06). Throughout this
241 manuscript we refer to the dry air mole fraction of CH_2Cl_2 as 'concentrations' to increase the
242 accessibility and readability of this manuscript.

243

244

245

246 The analytical precision during CARIBIC1 was 0.9% for the V.G. Autospec (based on repeat
 247 analysis of randomly selected samples, 1998-2002) and 2.4% for the Entech (based on repeat
 248 analyses of the working standard, 1999-2002). During CARIBIC2 the Entech system was managed
 249 by several operators and the analytical precision was calculated for each of these periods, again
 250 based on repeat analysis of randomly selected samples or repeat analysis of the working standards.
 251 Average precision was 3.42% between May 2005-September 2006, 4.0% between October 2006-
 252 October 2009, 5.5% between November 2009-October 2012 and 3.3% in November and December
 253 2012. Average precision for the Autospec system during CARIBIC2 was 0.48%. The final dataset
 254 used in this study is from 1998-2002 and 2005-2012.

255

256 **2.3 Ancillary measurements – CO, O₃ and back trajectories**

257

258 With a typical cruise altitude of 10-12 km CARIBIC intercepts air of both tropospheric and
 259 stratospheric origin. Data were labelled to indicate if they were of mainly tropospheric or
 260 stratospheric origin based on a chemical definition of the tropopause. O₃ is measured in-situ
 261 onboard the CARIBIC platform (see Sprung and Zahn, 2010) and therefore provides a measure of
 262 upper troposphere/lower stratosphere (UTLS) structure with a temporal and spatial resolution more
 263 suited to the discrete whole air samples than parameters derived from meteorological analyses, such
 264 as potential vorticity. Samples were classed as being predominantly stratospherically-influenced if
 265 the integrated O₃ mixing ratio for that sampling period was above a seasonal threshold determined
 266 by Eq (1), a method derived from CARIBIC data by Zahn & Brenninkmeijer (2003), confirmed by
 267 Thouret et al. (2006) and used as part of CARIBIC halocarbon analysis by Wisher et al. (2014).

268

$$269 \quad O_3^{tropopause} \text{ (in ppbv)} = 97 + 26 \sin \left[\frac{2\pi(\text{Day of Year}-30)}{365} \right] \quad (1)$$

270

271 A detailed discussion of O₃ as a chemical marker for the structure of the UTLS is provided by Zahn
 272 and Brenninkmeijer (2003) and Sprung and Zahn (2010). Briefly, the extratropical O₃ chemical
 273 tropopause is observed around 100 ppbv O₃ and can be seen in changes in the relationship between
 274 O₃ and tropospheric tracers such as CO and acetone. Above the chemical tropopause, a compact
 275 ‘mixing line’ between O₃ and, for example, CO, denotes the mixing of tropospheric and
 276 stratospheric air in the extratropical tropopause layer (ExTL). The ExTL extends up to a maximum
 277 of 400-500 ppbv O₃, above which lies the lowermost stratosphere (LMS). Fig. 1 shows which
 278 samples were classed as being of predominantly tropospheric origin and which were stratospheric.
 279 As tropospheric trends in CH₂Cl₂ form the focus of this investigation, stratospherically-influenced
 280 samples (which comprised between ~6-40% of samples, depending on the region) were excluded

281 from the bulk of the discussion for each region. Vertical profiles incorporating stratospheric
282 samples are discussed in Sections 3.4 and 3.5.

283

284 CARIBIC measurements of CO were used during the analysis of CH₂Cl₂ measured on flights to
285 South Africa and India (Sections 3.2 and 3.3 respectively). Details of CO measurements can be
286 found in Brenninkmeijer et al. (1999) for CARIBIC1 and Scharffe et al. (2012) for CARIBIC2. For
287 comparison with the whole air samples the CO values (produced every 2 s) were integrated over
288 the sampling period of each whole air sample. Back trajectory analyses for CARIBIC flights are
289 provided by the Royal Netherlands Meteorological Institute (KNMI), further details can be found at
290 knmi.nl/samenw/campaign_support/CARIBIC/ or in Scheele et al. (1996). The trajectory model
291 used European Centre for Medium range Weather Forecasting (ECMWF) data at a 1°x1° resolution
292 to calculate both 5 day back trajectories at 3 minute intervals along the flight track and 8 day back
293 trajectories for the collection interval of each whole air sample. During the early CARIBIC flights
294 ECMWF ‘first guess’ fields were used to calculate the back trajectories, changing to re-analysis
295 data after September 2000.

296

297 **3. Results and discussion**

298

299 Between 1998 – 2012 CARIBIC flights covered a substantial area of the global free troposphere
300 (Fig. 1). However, for the purpose of this investigation several regions were selected and only the
301 data from these flights will be discussed. These regions and the rationale behind their selection are
302 described here. Firstly, a European region within a box spanning 40 to 55 °N and -10 to 20 °E
303 (Frankfurt Airport = 50.03 °N, 8.57 °E) was selected as it is the area with the greatest temporal
304 coverage. Secondly, routes to South Africa, India and across the North and Central Atlantic were
305 also chosen as these routes were traversed by CARIBIC over multiple years, allowing changes over
306 time to be observed in these regions. Finally, samples collected in the tropical region covering 25 °S
307 to 25 °N were used to investigate the concentration of CH₂Cl₂ in air masses with the potential to
308 enter the tropical tropopause layer (TTL). Further details of these five case studies can be found in
309 Table 1 and they are highlighted in Fig. 1. Throughout the manuscript mean values prefaced by ±
310 refer to the 1 sigma standard error associated with that mean value.

311

312

313

314

315

316 **3.1 Long-term time series of CH₂Cl₂ measured over Europe**

317

318 The CH₂Cl₂ time series of European CARIBIC and NOAA Mace Head data can be seen in Fig. 2a.
319 A fairly consistent seasonal cycle is observed inter-annually in the boundary layer air samples from
320 Mace Head whereas the CARIBIC data show greater variability. This variability in the CARIBIC
321 data is mainly because these samples represent a wide variety of air masses sampled over a large
322 area (Fig. 2c) compared to clean-sector air sampled at Mace Head (Section 2.2). Analysis of back
323 trajectories indicates that air sampled by CARIBIC over Europe originates from a large NH
324 geographical region, including industrial areas where high emission ‘pollution’ events may occur as
325 well as contrasting regions where pristine tropospheric air masses are sampled. In contrast, the
326 Mace Head site commonly samples clean sector air. Although a previous study involving data
327 collected by aircraft at an average altitude of 4 km (Miller et al., 2012) observed seasonality in
328 atmospheric concentrations of CH₂Cl₂ we do not see a strong seasonal pattern at 10-12 km in our
329 more sporadic dataset. Further analysis, discussed in subsequent sections, will highlight the
330 importance of strong source regions (e.g. India and Southeast Asia) on observed CH₂Cl₂
331 concentrations in the mid and upper troposphere.

332

333 The trend in European observations of CH₂Cl₂ is shown in Fig. 2b. Error bars represent the 1σ
334 variation associated with the mean of all tropospheric samples taken within each year (hereafter be
335 referred to as the annual tropospheric value). As seen in Fig. 2a, only a small number of NOAA
336 samples were collected in the first few years of the dataset. Due to this small sample size, biases,
337 for example the influence of seasonality, could be introduced (see Table 3 for seasonal
338 distributions). This adds an additional, unquantified uncertainty to these annual values. To account
339 for this, data from Mace Head can be compared to data collected at other NOAA NH sites such as
340 Barrow, Alaska. Data from Barrow show a very similar pattern to those from Mace Head and
341 support the trend seen at Mace Head (data not shown but available from
342 <http://www.esrl.noaa.gov/gmd/hats/gases/CH2Cl2.html> and published in Montzka et al., 2011a).
343 Determining trends for the first few years of the database is hard due to the reduced data coverage.
344 However, NOAA data covers the whole year from 2003 onward (Fig. 2a).

345

346

347

348

349

350

351 The NOAA Mace Head data show no trend between 2003-2006 (linear fit is displayed in Fig. 2b)
352 with a steadily increasing trend from 2006. Despite the 1σ annual error bars being relatively large,
353 due to the seasonal variation seen at the Mace Head boundary layer site, a linear fit for the NOAA
354 data between 2006-2012 shows a strong positive correlation (see Fig. 2b, $r^2=0.97$). The increase
355 between the mean of all values collected within the first five years (1998-2002) and the final four
356 years (2009-2012) of the NOAA dataset was from 32.9 ppt ($\sigma=5.4$, sample size, $n=28$) to 45.7 ppt
357 ($\sigma=6.1$, $n=88$), an increase of ~ 13 ppt. A test of the robustness of the trend is to compare the change
358 from 2003-2004 (the first period with coverage across the entire year) and 2011-2012. During this
359 period CH_2Cl_2 increased from 35.6 ppt ($\sigma=5.1$, $n=48$) to 47.0 ppt ($\sigma=6.5$, $n=45$), an increase of 13.5
360 ppt. CARIBIC data broadly mirror the increasing trend between 2006-2012, bearing in mind the
361 more sporadic nature of the dataset and the wider distribution of air masses sources, discussed
362 above. The increase between the mean of all values collected between 1998-2002 and 2009-2012
363 was also similar to that seen at Mace Head, increasing from 24.6 ppt ($\sigma=4.3$, $n=21$) to 38.6 ppt
364 ($\sigma=8.4$, $n=49$) an increase of 14 ppt.

365

366 Whilst the overall trends are similar, mean annual values are higher at Mace Head (Fig. 2b). This is
367 likely to be because the NOAA samples were collected at a lower altitude than the CARIBIC
368 samples. Calibration scales between NOAA and UEA compare well, as described in Section 2 and
369 the Supplementary Information. Vertical profiles of CH_2Cl_2 are discussed in Sections 3.4 and 3.5.

370

371 Flight-based measurements in the NH were made by Simpson et al. (2011) (comparative data from
372 the literature is outlined in Table 2 for all regions). Although they flew up to 12 km their flight
373 altitudes were generally lower than CARIBIC (0.8-4.7 km). They reported a 2008 summer average
374 of 35.8 ± 2.9 ppt over Canada and Greenland. CARIBIC mean values for the 3 summers around this
375 time (2007, 2008 and 2009) were around 35, 27 and 37 ppt respectively, however as sample sizes
376 were small ($n=6$, 4 and 6 respectively) we combined these three summer periods to obtain a mean
377 for summers 2007-2009 of 33.9 ± 2.2 ppt. Our value is similar to that of Simpson et al., the higher
378 values over industrial Europe possibly offsetting some of the decrease we would expect with
379 altitude.

380

381

382

383

384

385

386 **3.2 Flights to Africa – investigating biomass burning emissions and NH:SH gradients**

387

388 Flights to South Africa (Table 1) allow us to investigate the NH:SH gradient in CH₂Cl₂, see Fig. 3a.
389 A strong latitudinal gradient is observed, in accordance with a strong industrial NH source of
390 CH₂Cl₂. The increase is largest over the northern section of the flight route, which crosses Europe.
391 We have a limited dataset (n=3) for the section of the flight route that crosses Europe (here defined
392 as > 30 °N to provide a clear delineation between samples taken over Africa and those taken within
393 our European box, see Fig. 1) and so we do not wish to quantify an increase over time, but from the
394 limited data available it is similar to that seen for our European box in Section 3.1. During the
395 previous peak in CH₂Cl₂ concentrations (around 1990, see Section 1) a difference of ~18 ppt
396 between NH and SH average concentrations was observed in the Atlantic region by Koppmann et
397 al. (1993) (Table 2). Whilst our results do not provide full SH coverage, and so cannot be used to
398 estimate a NH:SH ratio, they do show an increasing latitudinal variation indicative of increasing
399 NH industrial activity with respect to CH₂Cl₂.

400

401 Annual tropospheric values are shown in Fig. 3b, separated into samples taken above and below
402 30 °N. The 44% increase seen at latitudes <30 °N is smaller than that seen over Europe, although
403 still statistically significant (Mann-Whitney test at p<0.001). Further details of the concentrations
404 observed above and below 30 °N are provided in Table 2. Inferring year-on-year trends is difficult
405 given the varying data coverage between years. However, the increase seen between 2009 and 2011
406 (Fig. 3b), along with the European dataset (Fig. 2), suggest that concentrations continue to increase
407 into the 2010s.

408

409

410

411

412

413

414

415

416

417

418

419

420

421 Despite the importance of biomass burning with respect to atmospheric trace gas emissions over
422 Africa (Roberts et al., 2009) no correlation ($r=0.14$, $p>0.05$) was observed between CH_2Cl_2 and the
423 common combustion tracer CO. Enhancements of CO, which commonly peak near the equator in
424 CARIBIC data (Umezawa et al., 2014), are predominantly from biomass burning sources. In
425 contrast to the latitudinal distribution of CO, CH_2Cl_2 decreased constantly from north to south (Fig.
426 3). Observations of CH_2Cl_2 along the CARIBIC flight track to South Africa appear to be dominated
427 by a strong NH source and subsequent decline towards lower latitudes, with little impact from
428 biomass burning. This observation fits with a recent study which saw no evidence for CH_2Cl_2
429 emissions in boreal biomass burning plumes, suggesting that previous calculations of CH_2Cl_2
430 emissions from biomass burning (e.g. Rudolph et al., 1995) were overestimates (Simpson et al.,
431 2011). Whilst emissions from boreal and tropical forest fires may differ, recent analysis of air
432 samples collected during flights over biomass burning events in the Brazilian rainforest also showed
433 no significant fire emissions of CH_2Cl_2 (A. Wisher, UEA, pers. comms.).

434

435 **3.3 Emissions of CH_2Cl_2 from India investigated during the Indian monsoon**

436

437 CARIBIC data collected during flights to India in 2008 have previously been used to demonstrate
438 the impact of the Indian/Asian Summer Monsoon (ASM) on UTLS trace gas concentrations (Baker
439 et al., 2011; 2012; Schuck et al., 2010). As these studies reported elevated concentrations of many
440 trace gases linked to the persistent convection and anticyclonic flow of the ASM we have divided
441 flights to India into ‘monsoon’ (July – September, inclusive) and ‘non-monsoon’ (rest of year) for
442 this study (Tables 1 and 2). Latitudinal distributions of CH_2Cl_2 along routes to Indian destinations
443 are shown in Fig. 4, displayed with the oldest flights at the top of the plot.

444

445 As the ASM was a particular focus of CARIBIC during 2008 we begin our discussion of Fig. 4
446 with these flights. A pronounced difference in the CH_2Cl_2 distribution along the latitudinal flight
447 track can be seen between monsoon and non-monsoon months. During the 2008 monsoon (Fig. 4d)
448 concentrations between $\sim 25\text{-}40^\circ\text{N}$ are elevated compared to non-monsoon months (Fig. 4c). During
449 non-monsoon months a relatively flat latitudinal distribution of CH_2Cl_2 is observed along the
450 majority of the flight path with some elevated concentrations at latitudes less than 20°N . Analysis
451 of back trajectories indicates that these elevated samples (Fig. 4c) probed air that had recently been
452 at low altitude over Southeast Asia. The pattern during the monsoon season is consistent with
453 previous CARIBIC studies, referenced above, which reported elevated concentrations of NMHCs,
454 methane and other compounds within $\sim 25\text{-}40^\circ\text{N}$ due to interception of air masses with influence
455 from the continental boundary layer.

456 The difference between monsoon and non-monsoon months can also be observed in the earlier
457 (CARIBIC1) data, although the monsoonal elevation between $\sim 25\text{-}40^\circ\text{N}$ (Fig. 4b) is superimposed
458 on a north-south latitudinal gradient more clearly seen outside of the monsoon season (Fig. 4a).
459 This north-south gradient is similar to that seen in the data from flights to South Africa. An
460 important feature of Fig. 4 is the shift in the dominant latitudinal feature over time. In the 1998-
461 2001 period a north-south gradient, suggesting low CH_2Cl_2 emissions from India, is clear. In
462 contrast, very high concentrations at low latitudes are observed in later flights conducted in 2008
463 and 2011-2012 (Fig. 4e). High values at lower latitudes are in contrast with results for Africa
464 (Section 3.2) and to Central America (Section 3.4). These results suggest a shifting latitudinal
465 profile and an increase in emissions within the Indian region. One 2011 flight in particular showed
466 exceedingly high levels of CH_2Cl_2 (Fig. 4e). Analysis of back trajectories indicate these air masses
467 originated from a low altitude over India and Southeast Asia. This region is discussed further in
468 Section 3.5.

469

470 Increases were calculated for the period between 1998-2000 and 2008 and between 1998-2000 and
471 2011-2012. These are provided in Table 2 for both monsoon and non-monsoon months. However,
472 as was illustrated in our discussion of Fig. 4 (previous paragraph), during the non-monsoon months
473 we may sample air masses that originate from outside the Indian region. During the monsoon
474 months air masses within the monsoon anticyclone are much more isolated (full details provided
475 below) and so the increases during the monsoon period are more likely to represent changing
476 CH_2Cl_2 emissions from India and its neighbours. The increase between the 1998-2000 and 2008
477 monsoon periods was 15 ppt (69%, further details in Table 2). Measurements of air masses from the
478 Indian and south Asian region were made by Scheeren et al. (2002; 2003a) during two campaigns in
479 1999 and 2001. Their observations averaged 29 ($\sigma = 12$) ppt in 1999 and 23 ppt ($\sigma = 3$) in 2001 (see
480 Table 2). Their 2001 average, in particular, corresponds well to our early measurements over India
481 which averaged $\sim 20\text{-}22$ ppt.

482

483

484

485

486

487

488

489

490

491 As the strong convection associated with the ASM quickly elevates air masses from the Indian
 492 continental boundary layer and then isolates them within the monsoon anticyclone, UT mixing
 493 ratios over India during the monsoon are closely coupled to boundary layer emissions (Baker et al.,
 494 2011; 2012; Rauthe-Schöch, et al., 2014; Schuck et al., 2010). This makes the ASM an ideal case
 495 study for calculating emission estimates using the CARIBIC dataset. As the majority of CH₂Cl₂
 496 emissions are industrial we assume emissions do not change during the monsoon and so the
 497 increase in UT concentrations seen during this period can be attributed wholly to meteorological
 498 changes. This assumption is justified based on findings by Gentner et al. (2010) who showed an
 499 absence of seasonality in CH₂Cl₂ emissions based on measurements made in California and a study
 500 by McCulloch and Midgley (1996) who also reported an absence of seasonality based on their
 501 analysis of data on the global industrial use of CH₂Cl₂. Previous analyses of meteorological
 502 parameters during 2008 (Rauthe-Schöch, et al., 2014; Schuck et al., 2010) have demonstrated that
 503 the monsoon anticyclone was present in July-September. For emission estimates we take all
 504 tropospheric samples where both CO and CH₂Cl₂ were measured and which were collected <40 °N
 505 (for further explanation and justification of this method see Baker et al., 2011; Schuck et al., 2010)
 506 in July-September 2008, a total of 35 samples.

507

508 Emission estimates are often calculated using ratios whereby the compound of interest is compared
 509 to a compound with which it correlates and for which emissions are quantified, in this case CO. The
 510 emission estimate is based on the slope of the linear correlation between the two tracers using Eq. 2
 511 (where $E_{CH_2Cl_2}$ and E_{CO} are the emission estimates for CH₂Cl₂ and CO respectively).

512

$$513 \quad E_{CH_2Cl_2} = E_{CO} \times \left(\frac{\Delta CH_2Cl_2}{\Delta CO} \right) \quad (2)$$

514

515 The CH₂Cl₂ vs. CO correlation within the monsoon (<40 °N, July-September 2008) can be seen in
 516 Fig. 5a. The correlation has a statistically significant (Pearson's correlation coefficient, p<0.05) r
 517 value of 0.62. Correlations for individual months are also shown in Fig. 5a. No statistical difference
 518 (Fisher's z test with a z-crit. value of 0.05) exists between the slopes for individual months,
 519 allowing us to use the slope of the correlation for the whole ASM period for our emission estimate.
 520 Table 4 includes $\Delta CH_2Cl_2/\Delta CO$ values from this study as well as a range of published values from a
 521 variety of sources. Lower ratios are seen for wildfire and biomass burning plumes, with higher
 522 ratios (more similar to the ones we observed) for urban (likely industrial) emissions.

523

524

525

526 Before discussing our emission estimates we provide details of the assumptions and potential errors
527 associated with this method and our treatment of these factors. Firstly, this method assumes that the
528 two compounds share a common, dominant source and/or that emissions are co-located. Whilst
529 CH₂Cl₂ is of predominantly industrial origin (see Section 1) with emissions likely to be dominated
530 by areas of heavy anthropogenic influence e.g. cities CO has a more diffuse source. It has a large
531 combustion source which, in India, is dominated by the burning of biofuels and biomass (Dickerson
532 et al., 2002). Despite this, we believe CO provides the best option for emission estimates in this
533 region. On the scale of a regional emission estimate, CO and CH₂Cl₂ sources are co-located: both
534 show strong signatures from the Indian subcontinent where it is known that air masses sampled
535 within the monsoon anticyclone have likely originated from. CO emissions are also well quantified,
536 and comparisons between CO and anthropogenic chlorocarbons, including CH₂Cl₂, have also been
537 conducted in several other studies including Gentner et al. (2010); Millet et al. (2009); Simmonds et
538 al. (2006) and Palmer et al. (2003) (Table 4). Schuck et al. (2010) discussed the use of SF₆ as a
539 tracer. However, its extremely patchy distribution (strong point sources) results in a poor correlation
540 with CH₂Cl₂ and a poorer representation of the Indian monsoon plume.

541

542

543

544

545

546

547

548

549

550

551

552

553

554

555

556

557

558

559

560

561 To further support the suitability of the CH_2Cl_2 -CO ratio for estimating CH_2Cl_2 emissions we
562 describe two analyses which demonstrate that the variability we observe is due to recent emissions,
563 as opposed to variations in transport time or route prior to sampling. Firstly, we compared the
564 $\Delta\text{CH}_2\text{Cl}_2/\Delta\text{CO}$ value from our sample set ($n=35$) to the $\Delta\text{CH}_2\text{Cl}_2/\Delta\text{CO}$ value obtained from a
565 smaller dataset based on the method used in Baker et al. (2011). Baker et al., when performing
566 emission estimates for the same CARIBIC 2008 monsoon dataset, minimised the influence of
567 variability with respect to processing or other transport effects by selecting a dataset that included
568 only those samples whose back trajectories indicated low level (pressure >600 hPa) contact within
569 the monsoon anticyclone in the previous 5 days ($n=15$). Comparing this subset of samples to our
570 full sample set gives a very similar $\Delta\text{CH}_2\text{Cl}_2/\Delta\text{CO}$ and r value. The $\Delta\text{CH}_2\text{Cl}_2/\Delta\text{CO}$ and r values for
571 our dataset are shown in Table 4 and for the Baker et al. subset the age corrected slope was 4.9×10^{-4}
572 ($\pm 8.7 \times 10^{-5}$) and $r=0.67$. The similarity between the two values suggests that the correlation observed
573 in our dataset (Fig. 5) is influenced by local emissions and not differences in transport times or
574 source regions. This is supported by a second method in which we compared the CH_2Cl_2 vs. CO
575 correlation for the ASM samples with the correlation calculated for samples taken within the same
576 $14\text{-}40^\circ\text{N}$ latitudinal band but along flight routes to Africa (Section 3.2) and across the Atlantic
577 (Section 3.4). The correlation for the Africa and Atlantic flights are much weaker and do not show
578 the same dynamical range as the correlation for the India data. This supports our assumption that
579 samples taken during the ASM provide a unique correlation that represents local emissions due to
580 the rapid convection and isolation that occurs within the monsoon system.

581
582 Secondly, there are errors and assumptions associated with the measured emission ratio. This
583 includes the assumption that the emission ratio measured by CARIBIC is similar to that at the
584 source, i.e. it has not been affected by dilution and/or photochemical/chemical loss processes. We
585 believe this assumption to be valid with respect to dilution based on analysis conducted by Baker et
586 al. (2011) on the same CARIBIC dataset as used in this manuscript. Baker et al. (2011) reported an
587 i -butane/ n -butane ratio in the ASM of 0.77 ± 0.07 pptv pptv $^{-1}$, suggesting that the invariability of
588 this ratio provided evidence of minimal dilution. A broader investigation of the ASM by Randel and
589 Park (2006) using back trajectory models found that 70% of parcels initialised within the
590 anticyclone were still there after 10 days.

591

592

593

594

595

596 Dilution is also considered in our discussion of the validity of our ratio with respect to the transport
 597 time between emission source and sampling (previous paragraph), assuming variations in transport
 598 time lead to variations in the degree of mixing, and in the bootstrapping error analysis of the
 599 $\Delta\text{CH}_2\text{Cl}_2/\Delta\text{CO}$ regression line (subsequent paragraph). With respect to photochemical loss
 600 processes we assume transport times from the boundary layer to our sampling altitude of around 4
 601 days based on Baker et al. (2011). Within this time, CH_2Cl_2 , with a lifetime of around 5 months,
 602 does not experience large losses. However, the lifetime of CO (~2 weeks in mid latitude summer
 603 (Scharffe et al., 2012 referencing Warneck, 1988) is short enough that concentration changes are
 604 likely to have occurred during this time and so we age-correct our emission ratios with respect to
 605 CO using Eq. 3, a method used by both Baker et al. (2011) and Scheeren et al. (2002). Here, the
 606 emission ratio at time 0, ER_0 , is related to the emission ratio at time t, ER_t , by accounting for the
 607 change in time, Δt (4 days), the reaction rates, k, of CO and CH_2Cl_2 with OH at 298 K and the
 608 average concentration of OH predicted at 20 °N and 500 hPa (estimated uncertainty of $\pm 25\%$). Both
 609 k_{CO} at $2.1 \times 10^{-13} \text{ cm}^3 \text{ molec}^{-1} \text{ s}^{-1}$ and $\langle [\text{OH}] \rangle$ at $2.48 \times 10^6 \text{ molec cm}^{-3}$ are taken from Baker et al.
 610 (2011, and refs. within) and $k_{\text{CH}_2\text{Cl}_2}$ at $1.1 \times 10^{-13} \text{ cm}^3 \text{ molec}^{-1} \text{ s}^{-1}$ from Villenave et al. (1997). This
 611 procedure leads to a correction in our emission ratio for the 2008 monsoon season of around -8%.

$$ER_0 = ER_t e^{(k_{\text{CO}} - k_{\text{CH}_2\text{Cl}_2}) \langle [\text{OH}] \rangle \Delta t} \quad (3)$$

612
613
614
615
616
617
618
619
620
621
622
623
624
625
626
627
628
629
630

631 Also associated with the emission ratio are errors arising during the calculation of the
632 $\Delta\text{CH}_2\text{Cl}_2/\Delta\text{CO}$ slope. These errors arise from two sources: (1) uncertainties in the analytical
633 measurements of both CH_2Cl_2 and CO (see Section 2) and (2) uncertainties associated with using a
634 slope calculated from a discrete set of samples to calculate a regional emission estimate. The errors
635 associated with (1) are small compared to those associated with (2), see Section 2.2, and so we use
636 (2), calculated using a bootstrapping procedure, to set bounds on our emission estimates. Using the
637 Wood (2003) bootstrapping procedure we resampled, with replacement, our CH_2Cl_2 and CO
638 datasets 10000 times, each time calculating $\Delta\text{CH}_2\text{Cl}_2/\Delta\text{CO}$. The output from the resampling
639 procedure provides a probability distribution for the slope of $\text{CH}_2\text{Cl}_2/\text{CO}$, allowing us to understand
640 how dependent $\Delta\text{CH}_2\text{Cl}_2/\Delta\text{CO}$ may be on the sampled data and allowing us to provide an idea of
641 the potential variation in $\Delta\text{CH}_2\text{Cl}_2/\Delta\text{CO}$. The bootstrapping procedure has been used to calculate a
642 possible range of emission values to aid the comparison between years. In the following text this
643 $\pm 1\sigma$ range is given in brackets following each emission estimate.

644

645 CO emissions for the Indian region are taken from the Emission Database for Global Atmospheric
646 Research (EDGAR) v. 4.2 (JRC & PBL, 2009). We include emissions from the following countries;
647 Bangladesh, Bhutan, India, Sri Lanka, Maldives, Nepal and Pakistan. EDGAR emissions are
648 provided per year and are split into categories including various industrial and domestic processes,
649 transport and biomass and biofuel burning. Baker et al. (2012) used the Global Fire Emission
650 Database (GFED, v.3.2, van der Werf et al., 2010) to show that CO emitted from biomass burning
651 was greatly reduced during the monsoon, accounting for around 0.5% of total annual CO fire
652 emissions during 2008. To account for this reduction, the EDGAR biomass burning emissions were
653 corrected for the effect of the monsoon using the GFED data and the method in Baker et al. (2012).
654 As we had no evidence that anthropogenic Indian CO emissions had seasonality we divided these
655 emissions evenly throughout the year. We believe any errors arising from this assumption are likely
656 to be within the general errors associated with the EDGAR emissions (see below), in particular due
657 to the dominance of burning as a source of CO in India (Dickerson et al., 2002). This method gave
658 an average monthly emission during the 2008 monsoon of $4.2 \text{ Tg CO month}^{-1}$. Maximum errors on
659 the EDGAR CO database are given as up to $\pm 50\%$ (Olivier et al., 1999), likely reduced by our
660 additional use of the GFED database. We do not consider the given error on the EDGAR data
661 further as the main objective of these emission estimates is to provide a comparison of CH_2Cl_2
662 emissions over time and we assume this error remains constant throughout the EDGAR database.

663

664

665

666 Using the 2008 CH₂Cl₂/CO slope (Table 4) and the EDGAR CO emissions of 4.2 Tg CO month⁻¹
667 gives an emission estimate of 1.7 (1.3-2.1) Gg CH₂Cl₂ month⁻¹ from the Indian region. As industrial
668 sources of CH₂Cl₂ have no seasonality we assume this emission rate is constant over the year and so
669 estimate that 20.3 (15.8-24.8) Gg of CH₂Cl₂ were emitted from the Indian region in 2008. The most
670 recent estimate of global emissions is 515 ±22 Gg yr⁻¹ given in Montzka et al. (2011b) which is
671 based on top down estimates from Simmonds et al. (2006) from data collected between 1999 and
672 2003. Considering the caveat that global emissions are likely to have increased since this figure was
673 published, our estimate for emissions from the Indian region in 2008 is roughly 5% of the global
674 total. These estimates are discussed further in Section 3.6.

675

676 CH₂Cl₂ emissions from the Indian subcontinent were also estimated for the 1998, 1999 and 2000
677 ASM seasons using the same analysis described above for 2008. Fig. 5b shows the CH₂Cl₂ vs. CO
678 correlation for 1998-2000, coloured by year. No significant difference (Fisher's z test with a z-crit.
679 value of 0.05) was observed between the three years but we consider the three years individually to
680 provide similar datasets for comparison with the 2008 dataset (with respect to sample size and
681 length of sampling period, see Table 2). EDGAR monthly CO emissions, modified to account for
682 reduced burning during the monsoon, as described above, were 4.1, 4.2 and 4.2 Tg CO month⁻¹ for
683 1998, 1999 and 2000 respectively. As CO has anthropogenic sources one may expect its emissions
684 to have increased over time, however the monthly emissions for 1998-2000 are similar to those for
685 2008. To investigate this result we compared the EDGAR data to three previous studies. EDGAR
686 monthly emissions compare well to those of Fortems-Cheiney et al. (2011) who reported relatively
687 stable CO emissions from South Asia between 2000 and 2010. EDGAR monthly emissions also
688 compare well to the GIS-based emission estimate of Dalvi et al. (2006) and the air pollutant
689 emission inventory of Streets et al. (2003) who estimated that CO emissions from India in 2000
690 were 69 and 63 Tg respectively, similar to the 66 Tg annual emission estimated from the EDGAR
691 database for 2000. We use only the EDGAR data in the subsequent emission estimates for
692 consistency with both our 2008 emission estimate as well as previous studies, referenced above.
693 The resulting annual CH₂Cl₂ emissions are estimated at 4.9 (2.7-7.2) Gg yr⁻¹ in 1998, 7.9 (5.1-10.8)
694 Gg yr⁻¹ in 1999 and 12.6 (10.8-14.4) Gg yr⁻¹ in 2000. Our emission estimates suggest that emissions
695 have increased significantly over time; from a range of 3-14 Gg in the late 1990s to around 16-25
696 Gg in 2008.

697

698

699

700

701 3.4 CH₂Cl₂ measured during flights across the Atlantic to Central America

702

703 The final flight route with the temporal resolution needed for identifying CH₂Cl₂ trends is across the
704 Atlantic to Central America (Cuba, the Dominican Republic and northern Venezuela). Fig. 6 shows
705 the distribution of CH₂Cl₂ against both latitude and longitude sampled on flights to these
706 destinations. The gradient along the flight tracks, shown in Fig. 6 as average values binned for
707 every 5° latitude and 10° longitude, show very little variation in the early years of the dataset (2001-
708 2002). For example, the average CH₂Cl₂ value in the 5 ° latitude bins varied between 20-25 ppt
709 along the entire transect. The mean CH₂Cl₂ concentration was 23.8 (σ 3.9, n=9) ppt between 50-
710 55 °N and 19.5 (σ 2.6, n=8) ppt between 20-25 °N. The latitudinal gradient increases over time and
711 can be seen in the binned mean values for 2009-2011 which is to be expected as the northern
712 section of the flight route is crosses western Europe (Section 3.1) Due to the smaller number of
713 samples collected at the far ends of the transect (e.g. n=5 and n=3 for the far northern and southern
714 bins during the 2009-2011 flights) we do not quantify the gradient along the flight track. However,
715 it is still less pronounced than the latitudinal gradients observed en route to Africa or India, likely
716 due to the influence of clean Atlantic air.

717

718 Annual tropospheric values (Fig. 6c) show an increase in time, as discussed in previous sections
719 although the magnitude of the increase is much smaller and within the levels of variation observed.
720 Unlike previous sections, where we had defined spatial and temporal regions (e.g. Europe, Indian
721 monsoon) for which to calculate CH₂Cl₂ increases, this flight route can provide an idea that we see
722 CH₂Cl₂ increases, albeit small (from 23.2 ppt (σ=3.6) to 32.0 ppt (σ=7.8)), even in cleaner air
723 masses from over the Atlantic and Central America. There is a lack of CH₂Cl₂ measurements in the
724 Central American region with which to compare the CARBIC data.

725

726 Quasi-vertical profiles of CH₂Cl₂ along this route can also provide information on changes in
727 CH₂Cl₂ over time. In Fig. 7 profiles of CH₂Cl₂ are plotted as a function of O₃, as described in
728 Section 2. To investigate changes over time, Fig. 7 shows CH₂Cl₂-O₃ profiles for 2000-2002, 2009-
729 2010 and 2011-2012. Samples within each of these two-year periods are distributed evenly across
730 many months and so it is unlikely that seasonal bias plays a role in the changes observed over time.
731 Between 400-500 ppbv O₃ (n=4 for each two year period) the median CH₂Cl₂ value increased from
732 11 ppt in 2001-2002 to 16.0 ppt in 2011-2012. However, due to the low sample number and the
733 high variability this increase is within the uncertainties of these averages.

734

735

736 3.5 Vertical profiles of CH₂Cl₂ in the tropics

737

738 Air in the TTL may move quasi-horizontally into the ExTL or the LMS, or vertically into the
739 stratospheric overworld. Despite the fact that only a portion of the air from the TTL moves into the
740 free stratosphere, for short-lived species rapid convective transport to the TTL followed by ascent to
741 the free stratosphere is the most efficient transport pathway to the stratosphere (Law and Sturges,
742 2007). With a common cruise altitude of 10-12 km, CARIBIC flies at the lower edge of the TTL,
743 which is commonly defined as covering a potential temperature, θ , region of between around 345 K
744 (~12 km) and 380 K (~17 km). For this reason, we present only an upper limit on the changing
745 input of CH₂Cl₂ into this important region.

746

747 All data sampled within the tropical latitude band of 25 °S to 25 °N (the distribution of which can
748 be seen in Fig. 1, with further information in Table 1) were plotted as quasi-vertical profiles relative
749 to θ in Fig. 8. A clear increase in the magnitude of high CH₂Cl₂ ‘pollution’ events can be seen.

750 Because of this skew, median values and the range (min-max) are given for each 5 K altitude bin. In
751 1998-2002 the median CH₂Cl₂ concentration between 345-350 K was 18.1 (13.4-25.0, n=20) ppt.
752 The median value within this altitude bin between 2009-2012 was 23.2 ppt with a range spanning
753 12.4 to 90.4 ppt (n=97). The increase in median values is modest due to the inclusion of the 2009-
754 2010 data (see Section 3.4). However, despite the variability there is a statistically significant
755 (Mann Whitney test, $p < 0.05$) difference between the CH₂Cl₂ concentration observed between 345-
756 350 K.

757

758

759

760

761

762 With the exception of 2009-2010, see Section 3.4, CH₂Cl₂ concentrations observed in this vertical
763 band increased over time, reaching 26.8 (12.4-90.4, n=63) ppt in 2011-2012. Other measurements
764 of CH₂Cl₂ within this region are sparse. In 1991-1992 Schauffler et al. (1993) measured a mean
765 CH₂Cl₂ concentration of 14.9 ($\sigma=1.1$, n=12) in the TTL between 15.3-17.2 km (366-409 K).

766 Schauffler’s average is lower than that seen in the early CARIBIC data, although this is likely to be
767 due to the fact that (1) their measurements were taken a few years earlier than CARIBIC; (2) their
768 measurements were taken at a higher altitude; (3) their suggestion that their mean value was biased
769 low due a high degree of mixing with stratospheric air during their sampling period. Point (3)
770 demonstrates the influence that stratospheric mixing may have in this region and may explain the

771 low values we observed in the 2009-2010 period (see also Section 3.4). Between 2009 and 2011
772 tropical CH₂Cl₂ measurements were made by the HIAPER Pole-to-Pole Observations (HIPPO)
773 project (Wofsy et al., 2012). The HIPPO database contains 20 samples taken within the latitude
774 band 0° ±25° and within the 345-350 K θ band. These values are reported on the NOAA scale and
775 are therefore comparable with CARIBIC data. The HIPPO results, an average CH₂Cl₂ value of 26.3
776 (15.9-49.8) ppt, compare well to the CARIBIC results discussed above.

777

778 The data in Fig. 8 have been coloured by sampling route, thus providing a rough indication of
779 possible air mass source regions. Of interest is the group of high values in Fig. 8e sampled on the
780 one flight made to Bangkok and Kuala Lumpur at the end of 2012. With the rise of industrial
781 activity in Asia it is likely that emissions of industrial solvent emissions have also increased.
782 Studies in China have shown exceedingly high ground level concentrations of CH₂Cl₂. For
783 example, a 2001 study in 45 different Chinese cities by Barletta et al. (2006) saw an urban average
784 of 226 ppt (σ 232) and individual occurrences of up to 3 ppb. It is possible that high levels are also
785 emitted in other industrial parts of Asia, although there are little, if any, ground-based
786 measurements to support this.

787

788

789

790

791

792

793

794

795

796

797 **3.6 Potential causes for increasing CH₂Cl₂**

798

799 One likely contributor to the increase in CH₂Cl₂ is the increasing use of hydrofluorocarbons (HFCs)
800 as replacements for ozone-depleting CFCs and HCFCs the production and consumption of which
801 are strictly controlled by the Montreal Protocol. Specifically, CH₂Cl₂ is used in the production of
802 difluoromethane, also known as HFC-32 (Ramanathan et al., 2004). HFC-32 is used in combination
803 with HFC-125 to make the refrigerant R410A, a direct replacement for HCFC-22. It is estimated
804 that about 96% of HFC-32 emissions are in the NH (McCulloch, 2004), where the majority of
805 production and consumption of this HFC is likely to occur. Recent analysis of archived and

806 AGAGE air samples shows that HFC-32 has increased from around 0.7 ppt, when the first
807 measurements were made in 2004, to around 6.2 ppt in 2012, with the growth rate reaching 17% yr⁻¹
808 in recent years (O'Doherty et al., 2014; Montzka et al., 2011b). As HFCs do not deplete
809 stratospheric ozone they are not controlled by the Montreal Protocol. However, they are potent
810 greenhouse gases and, as such, are covered by European legislation controlling their production,
811 consumption and emission. This legislation is likely to reduce CH₂Cl₂ emissions from HFC
812 production in Europe in the coming years. In contrast, it is expected that much of the future demand
813 for HFCs is likely to come from developing countries (Velders et al., 2009). The use of air
814 conditioning systems is growing rapidly in India (e.g. NRDC, 2013); it is the world's third largest
815 consumer of CH₂Cl₂ (IHS, 2014) and HFC-32 production plants have opened in recent years
816 (Daikin, 2012). A rapidly expanding air conditioning industry and increased consumption of
817 CH₂Cl₂ in India could at least partly explain the occurrence of high CH₂Cl₂ observations in the
818 latter years of the CARIBIC dataset (Section 3.3 and Fig. 4e). A shift in the main consumers and
819 emitters of HFCs is supported by O'Doherty et al. (2014) who suggest that East Asian emissions are
820 underestimated in some inventories (e.g. EDGAR) and that emissions from East Asia are growing
821 in importance.

822

823 There are other uses for CH₂Cl₂ which could be contributing to the increasing atmospheric
824 concentrations. Industrial sources include use in office (plastic) materials and electronics (Bin
825 Babar and Shareefdeen, 2014; Kowalska and Gierczak, 2012), the production and use of which is
826 increasing in developing nations such as India and those in south east Asia. A CH₂Cl₂ source from
827 municipal waste disposal (Majumdar and Srivastava, 2012) may be of particular importance for
828 India where mismanagement of waste disposal has been found to lead to high levels of fugitive
829 volatile organic compound emissions from waste disposal sites. CH₂Cl₂ is also used by the
830 pharmaceutical industry in drug preparation, where its use may be increasing as a replacement for
831 CCl₄ which is regulated by the Montreal Protocol (UNEP CAP, 2009).

832

833 The likely sources of increased CH₂Cl₂ emissions over the past decade suggest that India might be
834 an increasingly important source of industrial CH₂Cl₂ emissions, as seen in the CARIBIC dataset,
835 although its emissions are still small on a global scale. We estimate CH₂Cl₂ emissions from the
836 Indian region in 2008 to be in the region of 20.3 (15.8-24.8) Gg. This is similar to an estimate of 24
837 (16-33) Gg yr⁻¹ for 2005 USA emissions calculated by Millet et al. (2009). The latest global
838 estimate provided by the WMO (Montzka et al., 2011b) gave global emissions of 515 Gg yr⁻¹ for
839 1999-2003 based on Simmonds et al., 2006). Both the India and USA emissions are small fractions
840 of this total (which is a lower limit due to the time frame it was based upon and the increasing

841 emissions over time) suggesting that other regions contribute significantly. Significant growth in
842 industrial production and consumption of HFCs in Asia, in particular in China, was projected by
843 Velders et al. (2009), suggesting that these regions may be or may become important source regions
844 of CH_2Cl_2 and warrant further study.

845

846 **4. Conclusions**

847

848 Results from CARIBIC flights spanning a significant part of the world provide evidence that
849 CH_2Cl_2 has increased in the atmosphere since our measurements began in 1998, consistent with the
850 increase observed at a remote surface site, MHD. A summary of the increase seen in each region is
851 provided in Table 2. An increase of between 38% (Atlantic routes) to 69% (India monsoon route)
852 was observed, corresponding to an increase of between ~7-9 ppt in cleaner air masses, such as those
853 encountered on flights to South Africa and across the North and Central Atlantic and ~12-15 ppt in
854 air masses over industrial regions such as Europe and India. This increase was seen in the average
855 CH_2Cl_2 observations for each region, as well as in an increase in high concentration ‘pollution’
856 events (e.g. Figs. 4 and 8). The increase is most likely a result of increasing industrial use of
857 CH_2Cl_2 , such as its use as a feedstock for the production of HFC-32.

858

859 Our results show that CH_2Cl_2 emissions from the Indian subcontinent have increased two- to
860 fourfold in a decade (1998-2008). The annual emissions from the Indian region in 2008, at ~20 Gg,
861 are similar to those estimated for the USA in 2005. Other Asian regions may also prove to be
862 emitting large quantities of CH_2Cl_2 : from a limited dataset we suggest that Southeast Asia may be
863 an important source region. However, there is little in situ data available for this region and further
864 investigations are warranted.

865

866

867 Increases in CH_2Cl_2 in UT air masses with the potential to enter the TTL can also be observed in the
868 CARIBIC database. Whilst CH_2Cl_2 is only a minor contributor to stratospheric ozone depletion
869 many other chlorocarbons have stable (e.g. CH_3Cl , see Umezawa et al. (2014)) or decreasing (e.g.
870 CFCs, CH_3CCl_3) atmospheric abundances. As our data suggest that CH_2Cl_2 may still be increasing
871 in the atmosphere its relative importance may increase if this trend continues.

872

873 **Acknowledgements**

874 The authors would like to thank the CARIBIC team and associated partner institutions, Lufthansa
875 Airlines, Lufthansa Technik and Fraport for their work and support that has led to the success of

876 CARIBIC over many years. In particular we thank Andreas Zahn and colleagues for the O₃ data,
877 Dieter Scharffe for the CO data and Peter van Velthoven for the back trajectory information.
878 Thanks to Claus Koepfel, Dieter Scharffe, Stefan Weber and Martin Körner for facilitating the
879 operations of the container and TRAC samplers before, during and after flights. Early CARIBIC
880 samples were partly analysed at UEA by Georgina Sturrock. J. Laube acknowledges the support of
881 a NERC fellowship (number NE/I021918/1). The data available in the Supplementary Information
882 would not be possible without the staff at the Cape Grim station and at CSIRO GASLAB Aspendale
883 for collecting and maintaining the Cape Grim air archive and preparing the UEA flask and sub-
884 samples. SAM acknowledges the technical assistance of C. Siso, B. Hall, and B. Miller in making
885 NOAA flask measurements at MHD and other sites, and support, in part, by NOAA Climate
886 Program Office's AC4 Program. We also acknowledge CSIRO and the Bureau of Meteorology for
887 funding these activities.

888

889

890

891

892

893

894

895

896

897

898

899

900

901

902

903

904

905

906

907

908 **References**

909

910 Andreae, M. O. and Merlet, P.: Emission of trace gases and aerosols from biomass burning, *Global*
911 *Biogeochemical Cycles*, v.15(4), 955-966, doi:10.1029/2000GB001382, 2001.

912 Bin Babar, Z. and Shareefdeen, Z.: Management and control of air emissions from electronic
913 industries, *Clean Tech. Envir.*, 16(1), 69-77, doi:10.1007/s10098-013-0594-6, 2014.

914 Baker, A. K., Slemr, F. and Brenninkmeijer, C. A. M.: Analysis of non-methane hydrocarbons in air
915 samples collected aboard the CARIBIC passenger aircraft, *Atmos. Measure. Tech.*, 3, 311–321,
916 doi:10.5194/amt-3-311-2010, 2010.

- 917 Baker, A. K., Schuck, T. J., Slemr, F., Van Velthoven, P., Zahn, A. and Brenninkmeijer, C. A. M.:
918 Characterization of non-methane hydrocarbons in Asian summer monsoon outflow observed by the
919 CARIBIC aircraft, *Atmos. Chem. Phys.*, 11(2), 503–518, doi:10.5194/acp-11-503-2011, 2011.
- 920 Baker, A. K., Schuck, T. J., Brenninkmeijer, C. A. M., Rauthe-Schöch, A., Slemr, F., Van
921 Velthoven, P. F. J. and Lelieveld, J.: Estimating the contribution of monsoon-related biogenic
922 production to methane emissions from South Asia using CARIBIC observations, *Geophys. Res.
923 Lett.*, 39(L10813), doi:10.1029/2012GL051756, 2012.
- 924 Barletta, B., Meinardi, S., Simpson, I. J., Rowland, F. S., Chan, C.-Y., Wang, X., Zou, S., Chan, L.
925 Y. and Blake, D. R.: Ambient halocarbon mixing ratios in 45 Chinese cities, *Atmos. Environ.*, 40,
926 7706–7719, doi: 10.1016/j.atmosenv.2006.08.039, 2006.
- 927 Brenninkmeijer, C. A. M., Crutzen, P. J., Fischer, H., Güsten, H., Hans, W., Heinrich, G.,
928 Heintzenberg, J., Hermann, M., Immelmann, T., Kersting, D., Maiss, M., Nolle, M., Pitscheider, A.,
929 Pohlkamp, H., Scharffe, D., Specht, K. and Wiedensohler, A.: CARIBIC - Civil aircraft for global
930 measurement of trace gases and aerosols in the tropopause region, *J. Atmos. Ocean. Tech.*, 16,
931 1373–1383, doi:dx.doi.org/10.1175/1520-0426(1999)016<1373:CCAFGM>2.0.CO;2, 1999.
- 932 Brenninkmeijer, C. A. M., Crutzen, P., Boumard, F., Dauer, T., Dix, B., Ebinghaus, R., Filippi, D.,
933 Fischer, H., Franke, H., Frieß, U., Heintzenberg, J., Helleis, F., Hermann, M., Kock, H. H.,
934 Koepfel, C., Lelieveld, J., Leuenberger, M., Martinsson, B. G., Miemczyk, S., Moret, H. P.,
935 Nguyen, H. N., Nyfeler, P., Oram, D., O’Sullivan, D., Penkett, S., Platt, U., Pucek, M., Ramonet,
936 M., Randa, B., Reichelt, M., Rhee, T. S., Rohwer, J., Rosenfeld, K., Scharffe, D., Schlager, H.,
937 Schumann, U., Slemr, F., Sprung, D., Stock, P., Thaler, R., Valentino, F., Van Velthoven, P.,
938 Waibel, A., Wandel, A., Waschitschek, K., Wiedensohler, A., Xueref-Remy, I., Zahn, A., Zech, U.
939 and Ziereis, H.: Civil aircraft for the regular investigation of the atmosphere based on an
940 instrumented container: the new CARIBIC system, *Atmos. Chem. Phys.*, 7(2), 5277–5339,
941 doi:10.5194/acpd-7-5277-2007, 2007.
- 942 Cox, M. L., Sturrock, G. A., Fraser, P. J., Siems, S. T., Krummer, P. B. and O’Doherty, S.:
943 Regional sources of methyl chloride, chloroform and dichloromethane identified from AGAGE
944 observations at Cape Grim, Tasmania, 1998–2000, *J. Atmos. Chem.*, 45, 79–99,
945 doi:10.1023/A:1024022320985, 2003.
- 946 Cox, R. A., Derwent, R. G. and Eggleton, E. J.: Photochemical oxidation of halocarbons in the
947 troposphere, *Atmos. Environ.*, 10, 305–308, doi:dx.doi.org/10.1016/0004-6981(76)90170-0, 1976.
- 948 Daikin: World’s first commercialization of air conditioning equipment using next-generation
949 refrigerant HFC-32 by Daikin, [online] Available from: [http://www.daikinindia.com/media-
950 room/daikin-announcements.html?view=detail&n_id=10](http://www.daikinindia.com/media-room/daikin-announcements.html?view=detail&n_id=10) (Accessed 11 April 2014), 2012.
- 951 Dalvi, M., Beig, G., Patil, U., Kaginalkar, A., Sharma, C. and Mitra, A. P.: A GIS based
952 methodology for gridding of large-scale emission inventories: Application to carbon-monoxide
953 emissions over Indian region, *Atmos. Environ.*, 40, 2995–3007,
954 doi:10.1016/j.atmosenv.2006.01.013, 2006.
- 955 Dickerson, R. R., Andreae, M. O., Campos, T., Mayol-Bracero, O. L., Neusuess, C. and Streets, D.
956 G.: Analysis of black carbon and carbon monoxide observed over the Indian Ocean: Implications
957 for emissions and photochemistry, *J. Geophys. Res.*, 107(D19), doi:10.1029/2001JD000501, 2002.

- 958 European Chlorinated Solvent Association (E.C.S.A.): White Paper - methylene chloride. Available
959 from: http://www.eurochlor.org/media/12847/5-1-2-1_white_paper_methylene_chloride.pdf
960 (Accessed on: 30.08.14) 2007.
- 961 Fortems-Cheiney, A., Chevallier, F., Pison, I., Bousquet, P., Szopa, S., Deeter, M. N. and Clerbaux,
962 C.: Ten years of CO emissions as seen from Measurements of Pollution in the Troposphere
963 (MOPITT), *J. Geophys. Res.*, 116, D05304, doi:10.1029/2010JD014416, 2011.
- 964 Gautrois, M., Brauers, T., Koppmann, R., Rohrer, F., Stein, O. and Rudolph, J.: Seasonal variability
965 and trends of volatile organic compounds in the lower polar troposphere, *J. Geophys. Res.*,
966 108(D13), doi:10.1029/2002JD002765, 2003.
- 967 Gentner, D. R., Miller, A. M. and Goldstein, A. H.: Seasonal variability in anthropogenic
968 halocarbon emissions, *Env. Sci. Tech.*, 44(14), 5377–5382, doi:10.1021/es1005362, 2010.
- 969 Hall, B. D., Engel, A., Mühle, J., Elkins, J. W., Artuso, F., Atlas, E., Aydin, M., Blake, D., Brunke,
970 E.-G., Chiavarini, S., Fraser, P. J., Happell, J., Krummel, P. B., Levin, I., Loewenstein, M.,
971 Maione, M., Montzka, S. A., O'Doherty, S., Reimann, S., Rhoderick, G., Saltzman, E. S., Scheel,
972 H. E., Steele, L. P., Vollmer, M. K., Weiss, R. F., Worthy, D. and Yokouchi, Y.: Results from the
973 International Halocarbons in Air Comparison Experiment (IHALACE), *Atmos. Meas. Tech.*, 7,
974 469–490, 2014, doi:10.5194/amt-7-469-2014, 2014.
- 975 IHS: Chlorinated methanes. [online] Available from:
976 <http://www.ihs.com/products/chemical/planning/ceh/chlorinatedmethanes.aspx> (Accessed 13 May
977 2014), 2014.
- 978 JRC & PBL (European Commission Joint Research Centre, JRC, and the Netherlands
979 Environmental Assessment Agency, PBL): Emission Database for Global Atmospheric Research
980 (EDGAR), release version 4.0, Available from: <http://edgar.jrc.ec.europa.eu/>, 2009.
- 981 Koppmann, R., Johnen, F. J., Plass-Dulmer, C. and Rudolph, J.: Distribution of methyl chloride,
982 dichloromethane, trichloroethene and tetrachloroethene over the North and South Atlantic, *J.*
983 *Geophys. Res.*, 98(D11), 517–526, doi: 10.1029/93JD01864, 1993.
- 984 Kowalska, J. and Gierczak, T.: Qualitative and quantitative analyses of the halogenated volatile
985 organic compounds emitted from the office equipment items, *Indoor Built Environ.*, 22(6), 920–
986 931, doi:10.1177/1420326X12458299, 2012.
- 987 Laube, J. C., Martinerie, P., Witrant, E., Blunier, T., Schwander, J., Brenninkmeijer, C. A. M.,
988 Schuck, T. J., Bolder, M., Röckmann, T., Van der Veen, C., Bönisch, H., Engel, A., Mills, G. P.,
989 Newland, M. J., Oram, D. E., Reeves, C. E. and Sturges, W. T.: Accelerating growth of HFC-227ea
990 (1,1,1,2,3,3,3-heptafluoropropane) in the atmosphere, *Atmos. Chem. Phys.*, 10(13), 5903–5910,
991 doi:10.5194/acp-10-5903-2010, 2010.
- 992 Laube, J. C., Engel, A., Bönisch, H., Möbius, T., Worton, D. R., Sturges, W. T., Grunow, K. and
993 Schmidt, U.: Contribution of very short-lived organic substances to stratospheric chlorine and
994 bromine in the tropics – a case study, *Atmos. Chem. Phys.*, 8(3), 8491–8515, 2008.
- 995 Law, K. S., Sturges, W. T., Blake, D.R., Blake, N.J., Burkholder, J.B., Butler, J.H., Cox, R.A.,
996 Haynes, P.H., Ko, M.K.W., Kreher, K., Mari, C., Pfeilsticker, K., Plane, J.M.C., Salawitch, R.J.,
997 Schiller, C., Sinnhuber, B.-M., von Glasow, R., Warwick, N.J., Weubbles, D.J., Yvon-Lewis, S.A.,
998 Butz, A., Considine, D.B., Dorf, M., Froidevaux, L., Kovalenko, L.J., Livesey, N.J., Nassar, R.,

- 999 Sioris, C.E., Weisenstein, D.K.: Chapter 2. Halogenated Very Short-Lived Substances, in Scientific
1000 Assessment of Ozone Depletion: 2006, 2007.
- 1001 Le Canut, P., Andreae, M. O., Harris, G. W., Wienhold, F. G. and Zenker, T.: Airborne studies of
1002 emissions from savannah fires in southern Africa. 1. Aerosol emissions measured with a laser
1003 optical particle counter, *J. Geophys. Res.*, 101(D19), 23615-23630, doi:10.1029/95JD02610, 1996.
- 1004 Majumdar, D. and Srivastava, A.: Volatile organic compound emissions from municipal solid waste
1005 disposal sites: A case study of Mumbai, India, *JAPCA J. Air Waste Ma.*, 62(4), 398–407,
1006 doi:10.1080/10473289.2012.655405, 2012
- 1007 McCulloch, A.: Determination of comparative HCFC and HFC emission profiles for the foam and
1008 refrigeration sectors until 2015. Part 3: Total emissions and global atmospheric concentrations,
1009 Marbury Technical Consulting and University of Bristol, 2004.
- 1010 McCulloch, A. and Midgley, P. M.: The production and global distribution of emissions of
1011 trichloroethene, tetrachloroethene and dichloromethane over the period 1988–1992, *Atmos.*
1012 *Environ.*, 30(4), 601–608, doi:10.1016/1352-2310(09)50032-5, 1996.
- 1013 McCulloch, A., Aucott, M. L., Graedel, E., Kleinman, G., Midgley, P. M. and Li, Y.-F.: Industrial
1014 emissions of trichloroethene, tetrachloroethene and dichloromethane: Reactive Chlorine Emissions
1015 Inventory, *J. Geophys. Res.*, 104(D7), 8417–8427, doi: 10.1029/1999JD900011, 1999.
- 1016 Miller, J. B., Lehman, S. J., Montzka, S. A., Sweeney, C., Miller, B. R., Karion, A., Wolak, C.,
1017 Dlugokencky, E. J., Southon, J., Turnbull, J. C. and Tans, P. P.: Linking emissions of fossil fuel
1018 CO₂ and other anthropogenic trace gases using atmospheric ¹⁴CO₂, *J. Geophys. Res.*, 117(D08302),
1019 doi:10.1029/2011JD017048, 2012.
- 1020 Millet, D. B., Atlas, E. L., Blake, D. R., Blake, N. J., Diskin, G. S., Holloway, J. S., Hudman, R. C.,
1021 Meinardi, S., Ryerson, T. B. and Sachse, G. W.: Halocarbon emissions from the United States and
1022 Mexico and their global warming potential, *Env. Sci. Tech.*, 43(4), 1055–1060,
1023 doi:10.1021/es802146j CCC, 2009.
- 1024 Montzka, S. A., Krol, M., Blugokencky, E., Hall, B., Jöckel, P. and Lelieveld, J.: Small interannual
1025 variability of global atmospheric hydroxyl, *Science*, v.331(6013), 67-69,
1026 doi:10.1126/science.1197640, 2011a.
- 1027 Montzka, S. A., Reimann, S., Engel, A., Kruger, K., O’Doherty, S., Sturges, W. T., Blake, D., Dorf,
1028 M., Fraser, P., Friodevaux, L., Jucks, K., Kreher, K., Kurylo, M. J., Miller, J., Neilson, O.-J., Orkin,
1029 V. L., Prinn, R. G., Rhew, R., Santee, M. L., Stohl, A. and Verdonik, D.: Chapter 1. Ozone-
1030 Depleting Substances (ODSs) and Related Chemicals, in WMO Scientific Assessment of Ozone
1031 Depletion: 2010, 2011b.
- 1032 NRDC (National Resources Defense Council): Cooling India with less warming: The business case
1033 for phasing down HFCs in room and vehicle air conditioners [online] Available from:
1034 <http://www.nrdc.org/international/india/files/air-conditioner-efficiency-IP.pdf> (Accessed 11 April
1035 14), 2013.
- 1036 O’Doherty, S., Rigby, M., Mühle, J., Ivy, D. J., Miller, B. R., Young, D., Simmonds, P. G.,
1037 Reimann, S., Vollmer, M. K., Krummel, P. B., Fraser, P. J., Steele, L. P., Dunse, B., Salameh, P.
1038 K., Harth, C. M., Arnold, T., Weiss, R. F., Kim, J., Park, S., Li, S., Lunder, C., Hermansen, O.,
1039 Schmidbauer, N., Zhou, L. X., Yao, B., Wang, R. H. J., Manning, A. and Prinn, R. G.: Global

- 1040 emissions of HFC-143a (CH₃CF₃) and HFC-32 (CH₂F₂) from in situ and air archive atmospheric
1041 observations, *Atmos. Chem. Phys.*, 14, 9249-9258, doi:10.5194/acp-14-9249-2014, 2014.
- 1042 Olivier, J. G. J., Bloos, J. P. J., Berdowski, J. J. M., Visschedijk, A. J. H. and Bouwman, A. F.: A
1043 1990 global emission inventory of anthropogenic sources of carbon monoxide on 1°×1° developed
1044 in the framework of EDGAR/GEIA, *Chemosphere - Global Change Science*, 1, 1-17,
1045 doi:10.1016/S1465-9972(99)00019-7, 1999.
- 1046 Palmer, P. I., Jacob, D. J., Mickley, L. J., Blake, D. R., Sachse, G. W., Fuelberg, H. E. and Kiley, C.
1047 M.: Eastern Asian emissions of anthropogenic halocarbons deduced from aircraft concentration
1048 data, *J. Geophys. Res.: Atmos.*, 108(D24), doi:10.1029/2003JD003591, 2003.
- 1049 Randel, W. J. and Park, M.: Deep convective influence on the Asian summer monsoon anticyclone
1050 and associated tracer variability observed with Atmospheric Infrared Sounder (AIRS), *J. Geophys.*
1051 *Res.*, 111(D12), D12314 (2006).
- 1052 Ramanathan, R., Anand, R., Jain, A. and Rao, J. M.: Process for the production of difluoromethane,
1053 United States Patent no. US 6,723,887 B2, 2004.
- 1054 Rauthe-Schöch, A., Baker, A. K., Schuck, T., Brenninkmeijer, C. A. M., Zahn, A., Herrmann, M.,
1055 Stratmann, G., Ziereis, H. and van Velthoven, P.: Pollution transport from the South Asian
1056 Monsoon anticyclone. To be submitted to *Atmospheric Chemistry and Physics Discussions*, 2014.
- 1057 Roberts, G., Wooster, M. J. and Lagoudakis, E.: Annual and diurnal African biomass burning
1058 temporal dynamics, *Biogeosciences*, 6(5), 849-866, doi:10.5194/bg-6-849-2009, 2009.
- 1059 Rudolph, J., Khedim, A., Koppmann, R. and Bonsang, B.: Field study of the emissions of methyl
1060 chloride and other halocarbons from biomass burning in western Africa, *J. Atmos. Chem.*, 22, 67-
1061 80, doi:10.1007/BF00708182, 1995.
- 1062 Scharffe, D., Slemr, F., Brenninkmeijer, C. A. M. and Zahn, A.: Carbon monoxide measurements
1063 onboard the CARIBIC passenger aircraft using UV resonance fluorescence, *Atmos. Measure. Tech.*,
1064 5, 1753-1760, doi: 10.5194/amt-5-1753-2012, 2012.
- 1065 Schaufli, S. M., Heidt, L. E., Pollock, W. H., Gilpin, T. M., Vedder, J. F., Solomon, S., Lueb, R.
1066 A. and Atlas, E. L.: Measurements of halogenated organic compounds near the tropical tropopause,
1067 *Geophys. Res. Lett.*, 20(22), 2567-2570, doi:10.1029/93GL02840, 1993.
- 1068 Scheele, M. P., Siegmund, P. C. and Van Velthoven, P. F. J.: Sensitivity of trajectories to data
1069 resolution and its dependence on the starting point: in or outside a tropopause fold, *Meteorol. Appl.*,
1070 3, 267-273, doi:10.1002/met.5060030308, 1996.
- 1071 Scheeren, H., Lelieveld, J., De Gouw, J. A., Van der Veen, C. and Fischer, H.: Methyl chloride and
1072 other chlorocarbons in polluted air during INDOEX, *J. Geophys. Res.*, 107(D19),
1073 doi:10.1029/2001JD001121, 2002.
- 1074 Scheeren, H. A., Lelieveld, J., Roelofs, G. J., Williams, J., Fischer, H., De Reus, M., De Gouw, J.
1075 A., Warneke, C., Holzinger, R., Schlager, H., Klüpfel, T., Bolder, M., Van der Veen, C. and
1076 Lawrence, M.: The impact of monsoon outflow from India and Southeast Asia in the upper
1077 troposphere over the eastern Mediterranean, *Atmos. Chem. Phys.*, 3, 1589-1608, doi:10.5194/acpd-
1078 3-2285-2003, 2003a.

- 1079 Schuck, T. J., Brenninkmeijer, C. A. M., Slemr, F., Xueref-Remy, I. and Zahn, A.: Greenhouse gas
1080 analysis of air samples collected onboard the CARIBIC passenger aircraft, *Atmos. Measure. Tech.*,
1081 2(2), 449–464, doi:10.5194/amt-2-449-2009, 2009.
- 1082 Schuck, T. J., Brenninkmeijer, C. A. M., Baker, A. K., Slemr, F., Velthoven, P. F. J. V. and Zahn,
1083 A.: Greenhouse gas relationships in the Indian summer monsoon plume measured by the CARIBIC
1084 passenger aircraft, *Atmos. Chem. Phys.*, 10(2), 3965–3984, doi:10.5194/acpd-10-2031-2010, 2010.
- 1085 Simmonds, P. G., Manning, A. J., Cunnold, D. M., McCulloch, A., O’Doherty, S., Derwent, R. G.,
1086 Krummel, P. B., Fraser, P. J., Dunse, B., Porter, L. W., Wang, R. H. J., Grealley, B. R., Miller, B. R.,
1087 Salameh, P., Weiss, R. F. and Prinn, R. G.: Global trends, seasonal cycles, and European emissions
1088 of dichloromethane, trichloroethene, and tetrachloroethene from the AGAGE observations at Mace
1089 Head, Ireland, and Cape Grim, Tasmania, *J. Geophys. Res.*, 111(D18304),
1090 doi:10.1029/2006JD007082, 2006.
- 1091 Simpson, I. J., Akagi, S. K., Barletta, B., Blake, N. J., Choi, Y., Diskin, G. S., Fried, A., Fuelberg,
1092 H. E., Meinardi, S., Rowland, F. S., Vay, S. A., Weinheimer, A. J., Wennberg, P. O., Wiebring, P.,
1093 Wisthaler, A., Yang, M., Yokelson, R. J. and Blake, D. R.: Boreal forest fire emissions in fresh
1094 Canadian smoke plumes: C1-C10 volatile organic compounds (VOCs), CO₂, CO, NO₂, NO, HCN
1095 and CH₃CN, *Atmos. Chem. Phys.*, 11(13), 6445–6463, doi:10.5194/acp-11-6445-2011, 2011.
- 1096 Sprung, D. and Zahn, A.: Acetone in the upper troposphere/lowermost stratosphere measured by the
1097 CARIBIC passenger aircraft: Distribution, seasonal cycle, and variability, *J. Geophys. Res.*,
1098 115(D16), D16301, doi:10.1029/2009JD012099, 2010.
- 1099 Streets, D. G., Bond, T. C., Carmichael, R., Fernandes, S. D., Fu, Q., He, D., Klimont, Z., Nelson,
1100 S. M., Tsai, N. Y., Wang, M. Q., Woo, J.-H. and Yarber, K. F.: An inventory of gaseous and
1101 primary aerosol emissions in Asia in the year 2000, *J. Geophys. Res.*, 108, D21,
1102 doi:10.1029/2002JD003093, 2003.
- 1103 Thouret, V., Cammas, J.-P., Sauvage, B., Athier, G., Zbinden, R., Nédélec, P., Simon, P. and
1104 Karcher, F.: Tropopause referenced ozone climatology and inter-annual variability (1994 – 2003)
1105 from the MOZAIC programme, *Atmos. Chem. Phys.*, 6(4) 1033-1051 (2006).
- 1106 Trudinger, C. M., Etheridge, D. M., Sturrock, G. A., Fraser, P. J., Krummer, P. B. and McCulloch,
1107 A.: Atmospheric histories of halocarbons from analysis of Antarctic firn air: Methyl bromide,
1108 methyl chloride, chloroform, and dichloromethane, *J. Geophys. Res.*, 109(D22), D22310,
1109 doi:10.1029/2004JD004932, 2004.
- 1110 Umezawa, T., Baker, A. K., Oram, D., Sauvage, C., O’Sullivan, D., Rauthe-Schöch, A., Montzka,
1111 S. A., Zahn, A. and Brenninkmeijer, C. A. M.: Methyl chloride in the upper troposphere observed
1112 by the CARIBIC passenger aircraft observatory: large-scale distributions and Asian summer
1113 monsoon outflow, *J. Geophys. Res.: Atmos.*, 119, doi:10.1002/2013JD021396, 2014.
- 1114 UNEP CAP (United Nations Environment Programme Compliance Assistance Programme): Fact
1115 Sheet no.26. Alternatives for Carbon Tetrachloride – CCl₄ (CTC) in laboratory and analytical uses,
1116 2009.
- 1117 Velders, G. J. M., Fahey, D. W., Daniel, J. S., McFarland, M. and Andersen, S. O.: The large
1118 contribution of projected HFC emissions to future climate forcing, *PNAS*, 106(27), 10949–54,
1119 doi:10.1073/pnas.0902817106, 2009.

- 1120 Villenave, E., Orkin, V. L., Huie, R. E. and Kurylo, M. J.: Rate Constant for the reaction of OH
1121 radicals with dichloromethane, *J. Phys. Chem.*, 101, 8513–8517, doi: 10.1021/jp9721614, 1997.
- 1122 Van der Werf, G. R., Randerson, J. T., Giglio, L., Collatz, G. J., Mu, M., Kasibhatla, P. S., Morton,
1123 D. C., DeFries, R. S., Jin, Y. and Van Leeuwen, T. T.: Global fire emissions and the contribution of
1124 deforestation, savannah, forest, agricultural, and peat fires (1997–2009), *Atmos. Chem. Phys.*,
1125 10(23), 11707–11735, doi:10.5194/acp-10-11707-2010, 2010.
- 1126 Warneck, P.: *Chemistry of the Natural Atmosphere*, Academic Press, London, 1988.
- 1127 Wisher, A., Oram, D. E., Laube, J. C., Mills, G. P., van Velthoven, P., Zahn, A. and
1128 Brenninkmeijer, C. A. M.: Very short-lived bromomethanes measured by the CARIBIC observatory
1129 over the North Atlantic, Africa and Southeast Asia during 2009–2013, *Atmos. Chem. Phys.*, 14(7),
1130 3557–3570, 2014.
- 1131 Wofsy, S. C., Daube, B. C., Jimenez, R., Kort, E., Pittman, J. V., Park, S., Commane, R., Xiang, B.,
1132 Santoni, G., Jacob, D., Fisher, J., Pickett-Heaps, C., Wang, H., Wecht, K., Wang, Q.-Q., Stephens,
1133 B. B., Shertz, S., Watt, A. S., Romashkin, P., Campos, T., Haggerty, J., Cooper, W. A., Rogers, D.,
1134 Beaton, S., Hendershot, R., Elkins, J. W., Fahey, D. W., Gao, R. S., Moore, F., Montzka, S. A.,
1135 Schwarz, J. P., Perring, A. E., Hurst, D., Miller, B. R., Sweeney, C., Oltmans, S., Nance, D., Hints,
1136 E., Dutton, G., Watts, L. A., Spackman, J. R., Rosenlof, K. H., Ray, E. A., Hall, B., Zondlo, M. A.,
1137 Diao, M., Keeling, R., Bent, J., Atlas, E. L., Lueb, R., Mahoney, M. J.: HIPPO Combined Discrete
1138 Flask and GC Sample GHG, Halo-, Hydrocarbon Data (R_20121129). Carbon Dioxide Information
1139 Analysis Center, Oak Ridge National Laboratory, Oak Ridge, Tennessee, U.S.A.
1140 http://dx.doi.org/10.3334/CDIAC/hippo_012 (Release 20121129), file
1141 [HIPPO_noaa_flask_allparams_merge_insitu_20121129](http://dx.doi.org/10.3334/CDIAC/hippo_012) (Accessed: 06 April 14), 2012.
- 1142 Wood, M.: Resample procedure for bootstrap confidence intervals, [online] Available from:
1143 <http://woodm.myweb.port.ac.uk/programs.htm> (Accessed 8 April 2014), 2003.
- 1144 Worton, D. R., Sturges, W. T., Schwander, J., Mulvaney, R., Barnola, J.-M. and Chappellaz, J.: 20th
1145 century trends and budget implications of chloroform and related tri- and dihalomethanes inferred
1146 from firn air, *Atmos. Chem. Phys.*, 6, 2847–2863, doi:10.5194/acp-6-2847-2006, 2006.
- 1147 Zahn, A. and Brenninkmeijer, C. A. M.: New Directions: A Chemical Tropopause Defined, *Atmos.*
1148 *Environ.*, 37(3), 439–440, doi:10.1016/S1352-2310(02)00901-9, 2003.

1149
1150
1151
1152
1153
1154
1155

TABLES

Table 1. A summary of CARIBIC data used in this study

Region	Temporal data coverage		Number of tropospheric (stratospheric*) samples
	Annual	Monthly	
Europe	Data collected 1998-2002 and 2005-2012 Min. coverage: n=1 in 1999 Max. coverage: n=16 in both 2009 and 2011	All months covered	123 (87)
Africa	2000, 2009-2011. Individual flights:	Mainly NH winter	140 (21)

	2000	May, July, Dec.	32 (4)
	2009	Mar., Oct.	47 (8)
	2010	Nov., Dec.	22 (6)
	2011	Jan., Feb., Mar.	39 (3)
India	Data collected 1998-2001, 2008, 2011 and 2012. The summer monsoon (July, Aug. and Sept.) was sampled in 1998, 1999, 2000 and 2008. In other years samples were only taken outside of the monsoon season.		295 (134)
	Monsoon	July, Aug., Sept.	105 (38)
	Non-monsoon	Rest of year	190 (95)
North and Central Atlantic	Data collected 2001-2002, 2007, 2009-2012	All months covered	282 (108)
Tropics	All data within $\pm 25^\circ$ of equator. All years included.	All months covered	539 (34)

*Stratospheric samples have been excluded from the analysis of most regions, see Section 2.

1156
1157
1158
1159
1160
1161
1162
1163
1164
1165
1166
1167
1168
1169
1170
1171
1172
1173
1174
1175
1176

Table 2. CH₂Cl₂ descriptive statistics for regions included in this study and a comparison to data from the existing literature

Study and Region	Time period*	Values [§] / ppt
This paper		
Europe		
CARIBIC data	(a) ^{&} 1998-2002 (b) 2009-2012 Increase (a→b)	\bar{x} =24.6 σ =4.3 n=21 \bar{x} =38.6 σ =8.4 n=49 14
Mace Head NOAA data	(a) 1998-2002 (b) 2003-2004 (c) 2009-2012 (d) 2011-2012 Increase (a→c) Increase (a→d)	\bar{x} =32.9 σ =5.4 n=28 \bar{x} =33.6 σ =5.1 n=48 \bar{x} =45.7 σ =6.1 n=88 \bar{x} =47.0 σ =6.5 n=45 13 13.5
Africa		
Above 30 °N	2000 2009-2011	\bar{x} =21.7 σ =1.3 n=3 \bar{x} =34.2 σ =7.6 n=23

Below 30 °N	2000 2009-2011 Increase	\bar{x} =15.8 σ =3.1, n=29 \bar{x} =22.7 σ =5.1 n=85 7
India		
Summer monsoon (July-Sept)	1998-2000 2008 Increase	\bar{x} =21.5 σ =3.8 n=56 \bar{x} =36.4 σ =9.4 n=50 15
Non-monsoon months	(a) 1998- 2000 (b) 2008 (c) 2011-2012 Increase (a→b) Increase (a→c)	\bar{x} =20.1 σ =4.9 n=81 \bar{x} =30.4 σ 9.7 n=62 33.4 σ =15.6 n=30 10 13
North and Central Atlantic	2000-2002 2009-2011	\bar{x} =23.2 σ 3.6 n=89 \bar{x} =32.0 σ 7.8 n=180
Other aircraft studies		
TTL (Schauffler et al., 1993)	1991-1992	\bar{x} =14.9, σ =1.1, n=12
Tropical Indian Ocean 1.2-12.5 km altitude (Scheeren et al., 2002)	1999	\bar{x} =29, SD= 12, n=71
ASM outflow, E. Mediterranean 6-13 km alt. (Scheeren et al., 2003a)	2001	\bar{x} =23, σ =3
Canada & Greenland, commonly 0.8-4.7 km but up to 12 km alt. (Simpson et al., 2011)	2008	\bar{x} =35.8 ±2.9
Tropics (0 ±25°), 345-350 K θ band (HIPPO, Wofsy et al., 2012)	2009-2011	\bar{x} =26.3, R=15.87-49.83, n=20
Ground-based		
Atlantic cruise 45 °N – 30 °S (Koppmann et al., 1993)	1989	
SH		\bar{x} =18 ±4
NH		\bar{x} =36 ±6 ppt
Alert, Canada (Gautrois et al., 2003)	1989-1996	\bar{x} =47.2 ±2, \tilde{x} =45.8 r=24.2-71.6
Cape Grim, Tasmania (Cox et al., 2003)	1998-2000	\bar{x} =8.9 ±0.2
Chinese cities (Barletta et al., 2006)	2001	
Background		\bar{x} =28, σ =4
Urban		\bar{x} =226, σ =232

1177 * Time period should be viewed alongside Table 3 which shows the seasonal distribution of samples.

1178 \bar{x} =mean, \tilde{x} = median, σ = standard deviation, R = range and n= number of samples.

1179 & see Section 3.1 for a description of the different time periods selected for Europe.

1180

1181 **Table 3. Seasonality of available CARIBIC data for regions included in this study*. Black**
 1182 **squares show that samples were taken during that month and the number refers to the**
 1183 **number of samples[§].**

Period ^a	Jan	Feb	Mar	Apr	May	Jun	Jul	Aug	Sep	Oct	Nov	Dec
Europe , CARIBIC												
1998-2001					3	6	2	4			1	
2009-2012	7	3	12	20	24	5	4	13	9	8	5	1
Mace Head NOAA												
1998-2001	1	1		1		1	3	4	1	3	1	
2003-2004	4	4	4	4	4	4	4	3	5	3	5	4
2009-2012	6	9	6	8	10	8	7	7	7	5	8	7
Africa >30 °N												
2000					1		1					1
2009-2011	3	3	8							4	4	2
Africa <30 °N												
2000					9		9					11
2009-2011	10	10	31							18	6	10
Atlantic/Central America												
2001-2002		11		20	17	9	11	10			11	
2009-2011	26		31	19	13	20	21	18		8	10	19

1184 *India is not included as focus is on summer monsoon and so seasonality throughout the whole year is not relevant.

1185 Tropical region not included due to reduced seasonality in the tropics. Samples sizes for both these regions can be found

1186 in Tables 1 and 2.

1187 [§] Samples are an average of 2 flask samples (NOAA) or at least two analyses of sample (UEA).

1188 ^a relates to any discrete time period mentioned in the text or Tables 1 and 2.

1189

1190 **Table 4. A comparison of enhancement ratios from this study (air mass age corrected) and**
 1191 **existing literature**

1192

Source	$\Delta \text{CH}_2\text{Cl}_2/\Delta \text{CO} / \text{mol mol}^{-1}$
India, summer monsoon period (this study)^a	
1998	$1.0 \times 10^{-4} (\pm 4.3 \times 10^{-5})$ r=0.69
1999	$1.6 \times 10^{-4} (\pm 6.4 \times 10^{-5})$ r=0.53
2000	$2.5 \times 10^{-4} (\pm 3.7 \times 10^{-5})$ r=0.86
2008	$4.0 \times 10^{-4} (8.7 \times 10^{-5})$ r=0.62
Other studies^b	
Biomass burning, Africa savanna, ground-based, 1991 ¹	2.5×10^{-5} (error = 26%) r=0.65
Wildfires, Cape Grim, ground-based, 1998-2004 ²	$< 1.6 \times 10^{-7}$
Asian pollution outflow, Bay of Bengal, boundary layer flights, 1999 ³	$4.4 \times 10^{-5} (\pm 4.7 \times 10^{-5})$ r=0.39
Urban, California, ground-based, 2005 ⁴	$3.1 \times 10^{-4} (\pm 3.0 \times 10^{-5})$ r=0.58-0.66
Urban, USA, boundary layer flights, 2004 ⁵	$2.4 \times 10^{-4} (1.8 \times 10^{-4} - 2.9 \times 10^{-4})$ r=0.56-0.83
Urban, Mexico, ground-based, 2006 ⁵	$1.9 \times 10^{-4} (1.1 \times 10^{-4} - 2.9 \times 10^{-4})$ r=0.43-0.81

1193 ^aCARIBIC fits are orthogonal distance regression fits using IGOR Pro software.

1194 ^bdescribed by: emission source, location, sampling location, year of study

1195 ¹(Rudolph et al., 1995); ²(Simmonds et al., 2006); ³(Scheeren et al., 2002); ⁴(Gentner et al., 2010); ⁵(Millet et
 1196 al., 2009).

1197

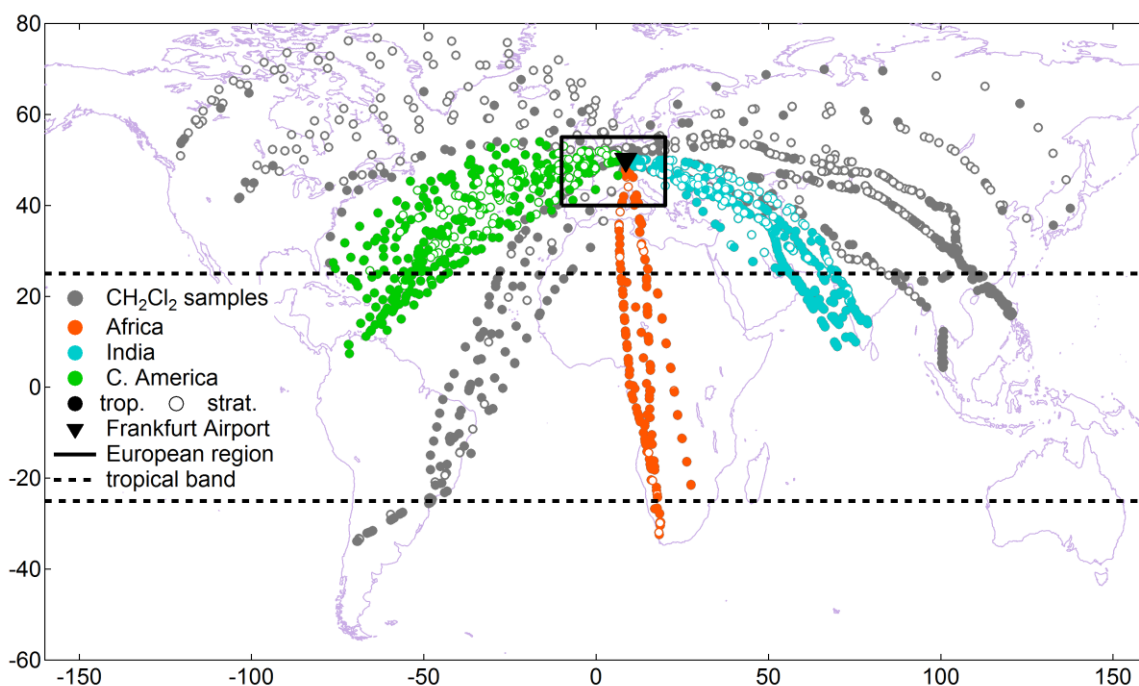
1198

1199

1200

1201

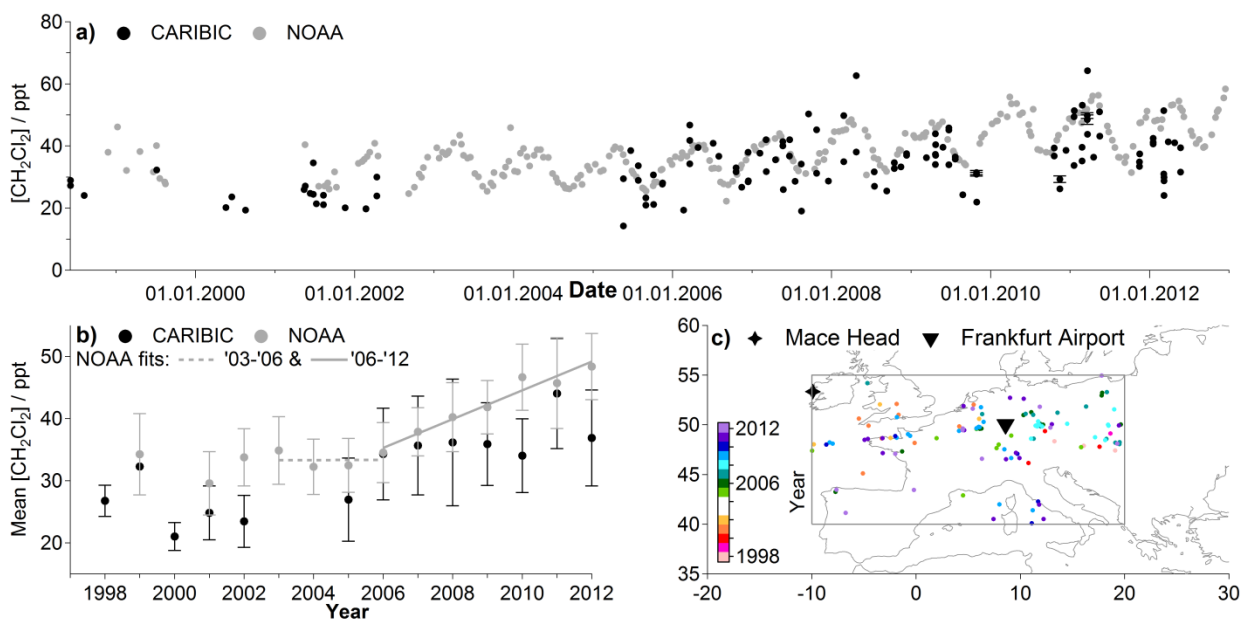
FIGURES



1202

1203 **Figure 1.** CARIBIC whole air samples analysed for CH_2Cl_2 between 1998-2002 and 2005-2012.

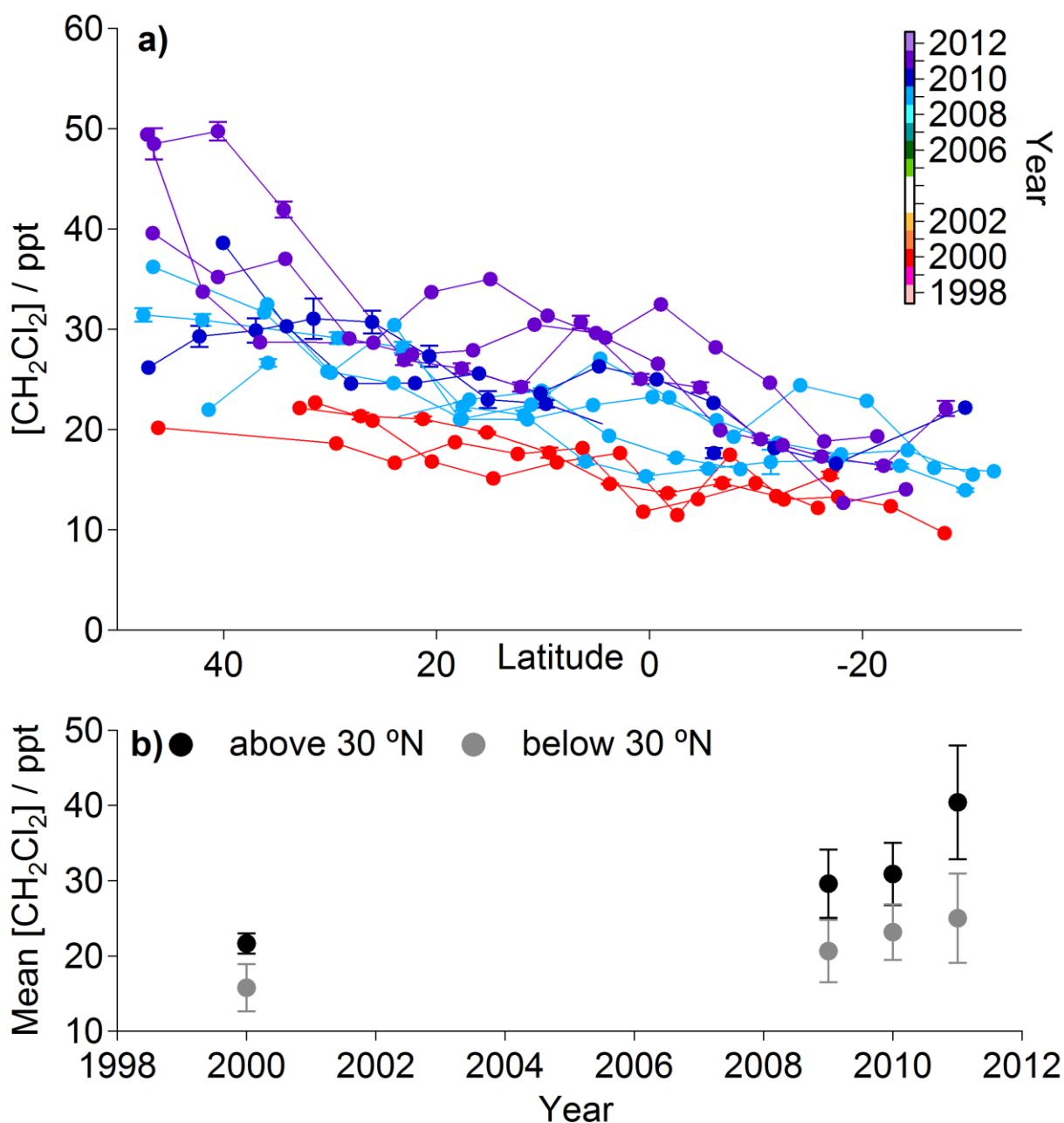
1204 The grey points show all the CH_2Cl_2 samples collected by CARIBIC during these periods. The
 1205 subset of data used in this study are also shown: (1) the samples within the European region
 1206 described in Section 3 are marked by the black box, (2) flight routes to Africa, India and Central
 1207 America are shown by coloured samples, see inset legend, and (3) samples within the tropical
 1208 region are delineated by the dashed lines. More details of the regions used in this study can be
 1209 found in Table 1. The identification of samples as tropospheric or stratospheric is described in
 1210 Section 2.



1211

1212 **Figure 2.** a) European CH_2Cl_2 time series from June 1998 to December 2012. Where a sample was
 1213 analysed multiple times an error bar is given based on the variation between these measurements,
 1214 see Section 2. b) The mean value of all CH_2Cl_2 values taken within this region for each year
 1215 ('annual tropospheric value'), shown separately for CARIBIC and NOAA Mace Head data, error
 1216 bars are 1σ . c) Geographical distribution of CARIBIC samples within the European region 40-
 1217 55 °N and -10-20 °E. Frankfurt Airport (CARIBIC2 base) and the NOAA sampling site at Mace
 1218 Head are also shown. Samples are coloured by year.

1219



1220

1221 **Figure 3.** a) Latitudinal distributions of CH_2Cl_2 observed during flights to South Africa where
 1222 colour = year (see inset colour bar, colour scale is consistent with Figs. 2, 4 and 6). Where multiple
 1223 measurements of the same sample have been made 1σ error bars are given, see Section 2. b) Annual
 1224 tropospheric values (see Fig. 2) with 1σ error bars. These average values have been split into
 1225 above and below 30 °N.

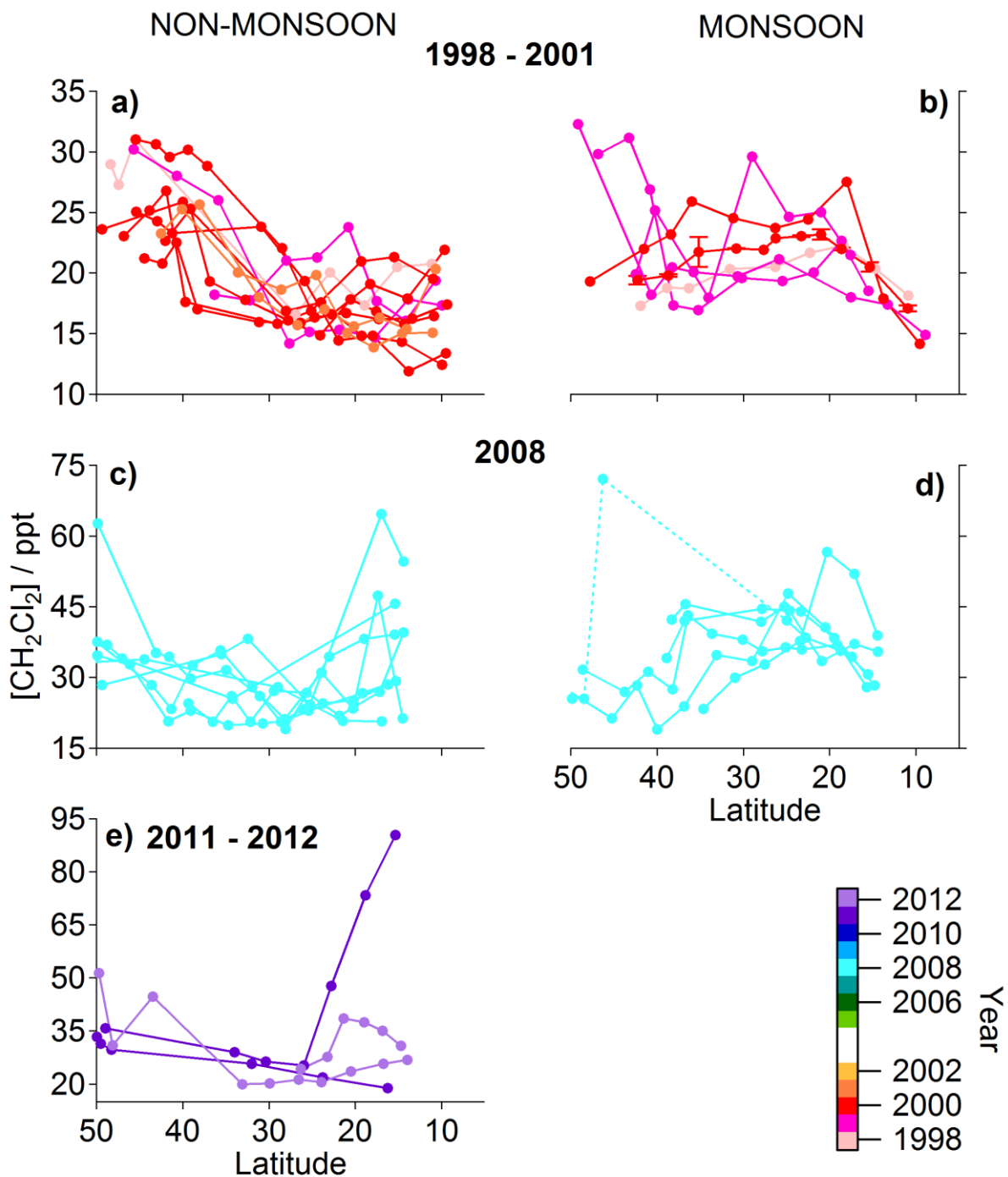
1226

1227

1228

1229

1230



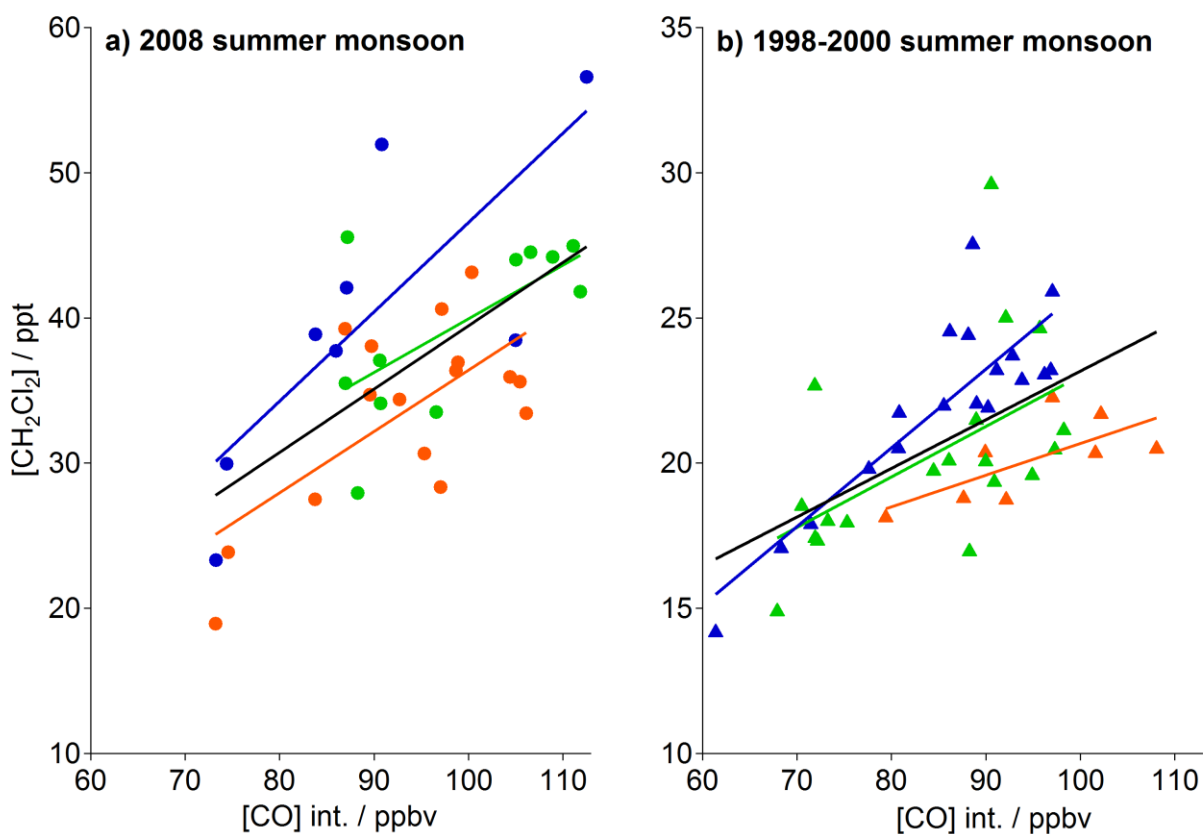
1231

1232 **Figure 4.** Latitudinal distributions of CH_2Cl_2 observed during flights to India for non-monsoon
 1233 months on the left and monsoon months (July, August, September) on the right where colour = year
 1234 (see inset colour bar, colour scale is consistent with Figs. 2, 4 and 6. Where multiple measurements
 1235 of the same sample have been made 1σ error bars are given, see Section 2.

1236

1237

1238



1239

1240 **Figure 5.** Correlation plots of CH_2Cl_2 and integrated CO (see Section 2) for a) the 2008 summer
 1241 monsoon period (coloured by individual months) and b) the early years of the CARIBIC India
 1242 dataset (coloured by individual years). Further details in Table 4.

1243

1244

1245

1246

1247

1248

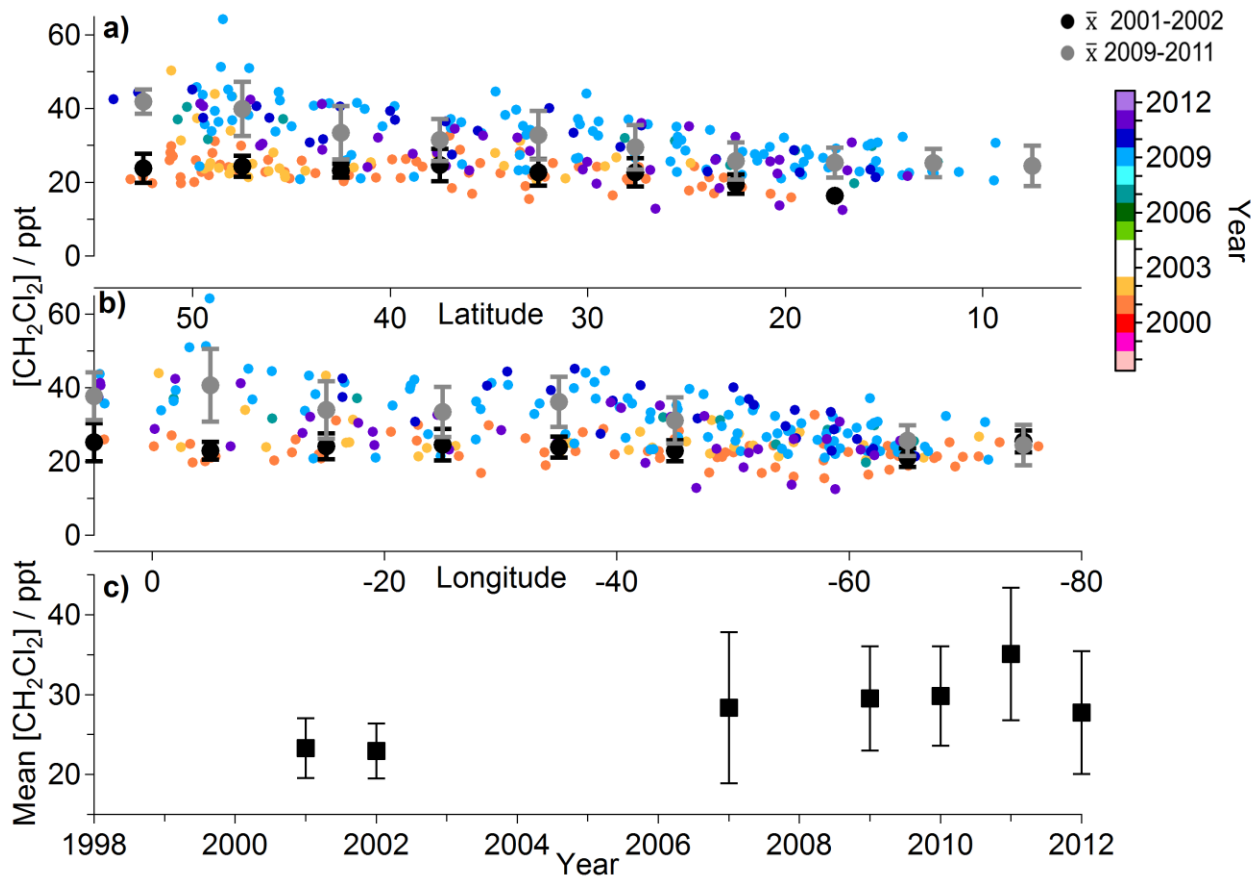
1249

1250

1251

1252

1253



1254
 1255 **Figure 6.** (a) Latitudinal and b) longitudinal distributions of CH_2Cl_2 along flight routes across the
 1256 North and Central Atlantic to Central America where colour = year (see inset colour bar, colour
 1257 scale is consistent with Figs. 2,4 and 6). Average, \bar{x} , values for 5° latitude and 10° longitude bins
 1258 are shown for 2001-2002 and 2009-2011 (see Section 3.4), error bars are the 1σ variation within
 1259 these bands. c) Annual tropospheric values (see Fig. 2) with 1σ error bars.

1260

1261

1262

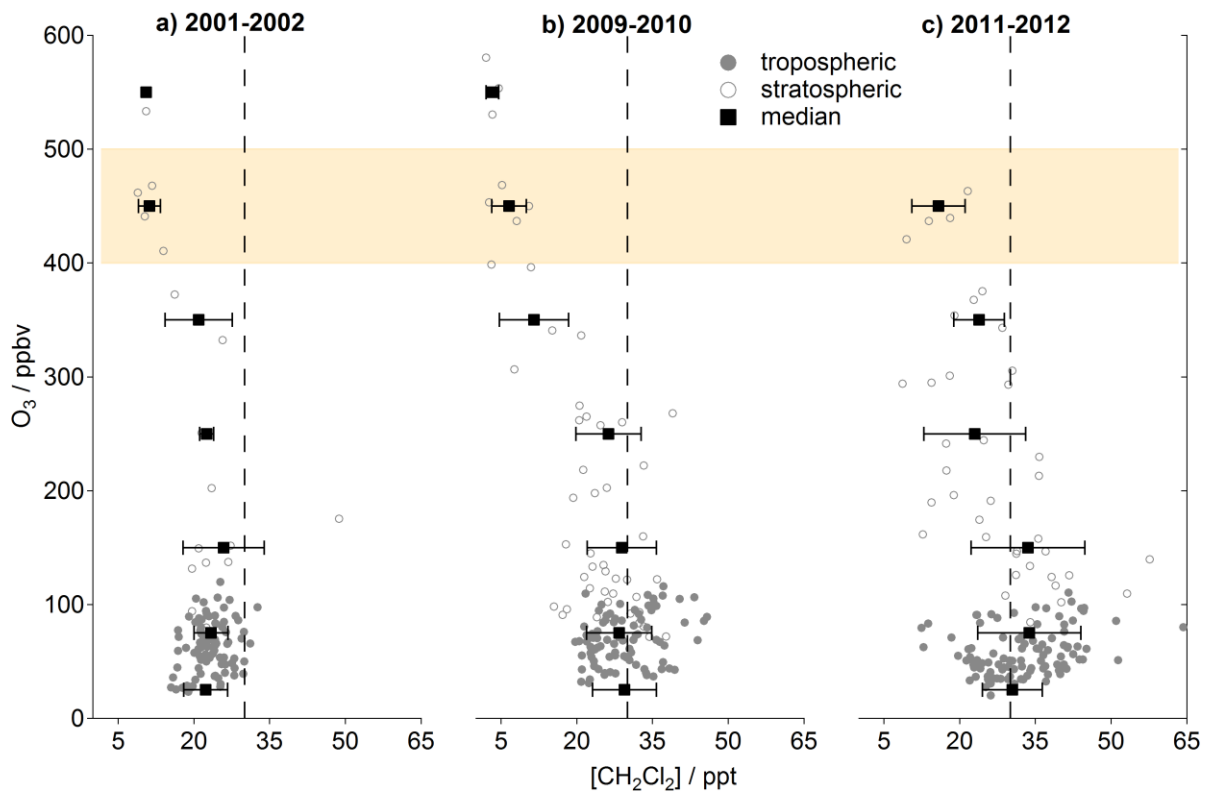
1263

1264

1265

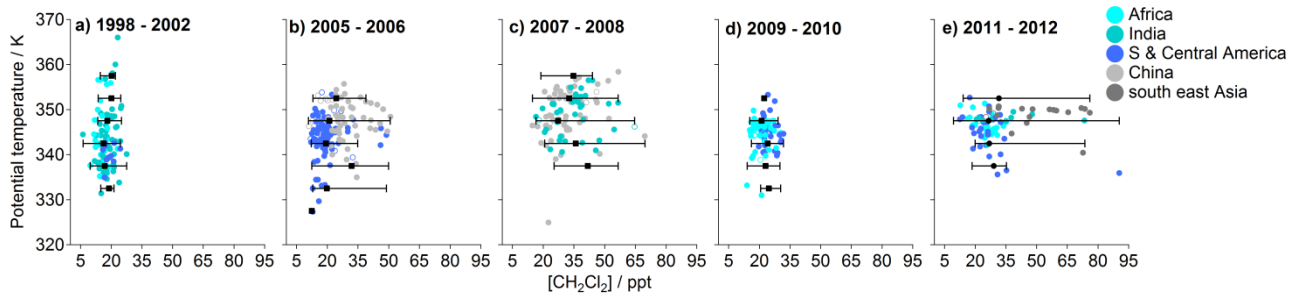
1266

1267



1268
 1269 **Figure 7.** Profiles of CH_2Cl_2 relative to O_3 from samples collected on flights across the North and
 1270 Central Atlantic to Central America. Median values are for 50 ppb O_3 bins between 0-100 ppbv and
 1271 100 ppbv O_3 bins above this, error bars are 1σ . The coloured band highlights the region between
 1272 400-500 ppbv O_3 discussed in Section 3.4. The dashed line represents 30 ppt of CH_2Cl_2 (see Section
 1273 1), provided as a visual marker to illustrate the shift over time to higher concentrations of CH_2Cl_2 .

1274



1275

1276 **Figure 8.** Profiles of CH_2Cl_2 relative to potential temperature for samples taken within the latitude
 1277 range $0^\circ \pm 25^\circ$. Median (error bars are range) values for 5 K bins are overlaid in black. Colour
 1278 represents flight route, as shown by the inset colour bar.